

Photoswitching Protein-XTEN Fusions as Injectable Optoacoustic Probes

Yishu Huang^{1,2†}, Mariia Stankevych^{1,2†}, Vipul Gujrati^{1,2}, Uwe Klemm^{1,2}, Azeem Mohammed^{1,2}, David Wiesner¹, Mara Saccomano³, Monica Tost⁴, Annette Feuchtinger⁴, Kanuj Mishra^{1,2*}, Oliver Bruns³, Arie Geerlof⁵, Vasilis Ntziachristos^{1,2} and Andre C. Stiel^{1,2,6*}

1: Institute of Biological and Medical Imaging, Bioengineering Center, Helmholtz Zentrum München, Neuherberg, Germany.

2: Chair of Biological Imaging, Central Institute for Translational Cancer Research (TranslaTUM), School of Medicine and Health & School of Computation, Information and Technology, Technical University of Munich, Munich, Germany.

3: Helmholtz Pioneer Campus, Helmholtz Zentrum München, Neuherberg, Germany.

4: Core Facility Pathology & Tissue Analytics, Helmholtz Zentrum München, Neuherberg, Germany

5: Protein Expression and Purification Facility, Institute of Structural Biology, Helmholtz Center Munich for Environmental Health, Neuherberg, Germany.

6: Protein Engineering for Superresolution Microscopy Lab, University of Regensburg, Regensburg, Germany

* Correspondence to: andre.stiel@helmholtz-munich.de or kanuj.mishra@tum.de

† These authors contributed equally

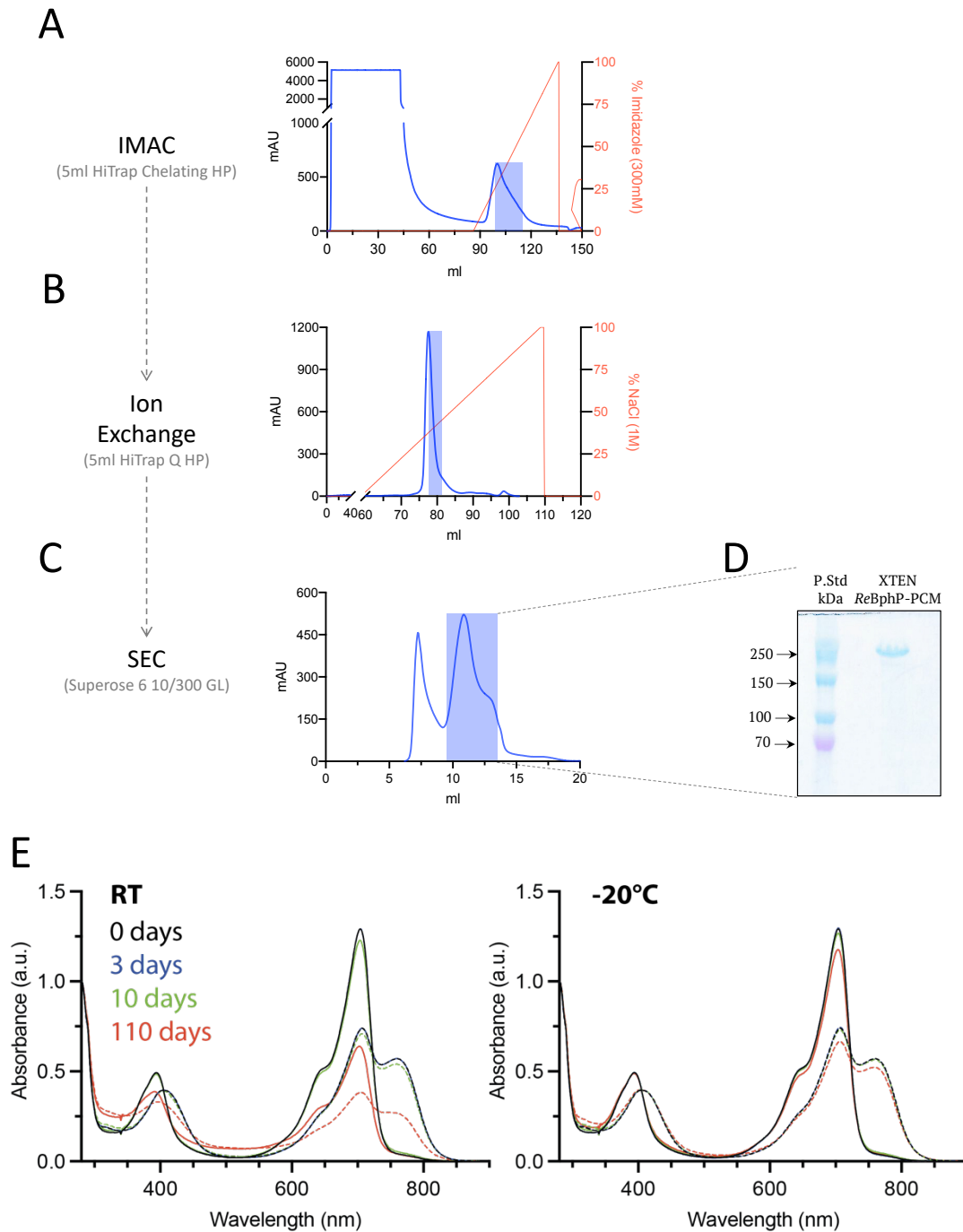
XTEN-ReBphP-PCM

MGGSPAGSPTSTEEGTSESATPESGPGTSTEPSEGSAPGSPAGSPTSTEEGTSTEPSEGSAPGTSTEPSEGSAPG
TSESATPESGPGSEPATSGSETPGSEPATSGSETPGSPAGSPTSTEEGTSESATPESGPGTSTEPSEGSAPGTST
EPSEGSAPGSPAGSPTSTEEGTSTEPSEGSAPGTSTEPSEGSAPGTSESATPESGPGTSTEPSEGSAPGTSESAT
PESGPGSEPATSGSETPGTSTEPSEGSAPGTSTEPSEGSAPGTSESATPESGPGTSESATPESGPGSPAGSPTST
EEGTSESATPESGPGSEPATSGSETPGTSESATPESGPGTSTEPSEGSAPGTSTEPSEGSAPGTSTEPSEGSAPG
TSTEPSEGSAPGTSTEPSEGSAPGTSTEPSEGSAPGSPAGSPTSTEEGTSTEPSEGSAPGTSESATPESGPGSEP
ATSGSETPGTSESATPESGPGSEPATSGSETPGTSESATPESGPGTSTEPSEGSAPGTSESATPESGPGSPAGSP
TSTEEGSPAGSPTSTEEGSPAGSPTSTEEGTSESATPESGPGTSTEPSEGSAPSGSGTSESATPESGPGSEPATSG
GSETPGTSESATPESGPGSEPATSGSETPGTSESATPESGPGTSTEPSEGSAPGSPAGSPTSTEEGTSESATPES
GPGSEPATSGSETPGTSESATPESGPGSPAGSPTSTEEGSPAGSPTSTEEGTSTEPSEGSAPGTSESATPESGPG
TSESATPESGPGTSESATPESGPGSEPATSGSETPGSEPATSGSETPGSPAGSPTSTEEGTSTEPSEGSAPGTST
EPSEGSAPGSEPATSGSETPGTSESATPESGPGTSTEPSEGSAPSSSSGSSSSGGSMSGTREPMDLTNC DREPIH
QLGAIQPFGLLQVSSDWIVTRASVNLAEFLGVTQADALGRPASTLIMPEALHTIRNKLTTLRGADVVERVFAIA
LTPDQSKFDVAVHFNESQVIEGERCQEDRRNAPSLSMRSMMSRLDQAETLEAFFREGARQARALTGFDRVMVYR
FDEGGSGEVVAEAARSIGSFLGLHYPASDIPVQARALYLRNLFRIIADVDAVPVPI LPERDEHGQPLDLSMSVL
RSVSPIHIEYLKNNMGV GASLSISIVVDGKLWGLFACHHYEPRLPSAQSRSTAELFGQMFASRLSRERRLALDYE
TKARRIADRLT SVADNASLLDDPAWLEALADAI PADGIGVWINGRLALAGIGPDKKNFASLVRHLNRNAGGRI
YAVDRLSQTYPDLEIDAVVAGMLAIPISRSRPRDYVVLFRQELVRTVVRWGGDPHKPVEYGPNGPRLTPRKSFEWS
ELVRGRSLPFTEAEQ RVAETIRVTLIEVVLRLTDEASMARQMANERQELLIAELNENLYFQCHHHHHHHH

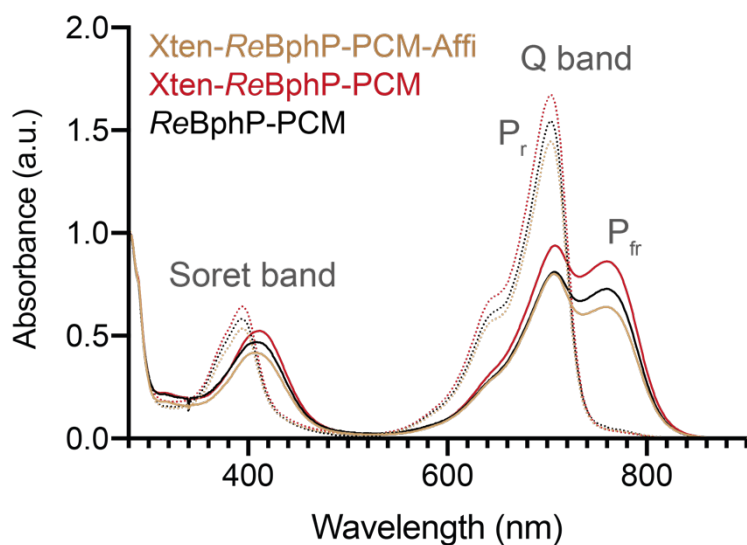
XTEN-ReBphP-PCM-Affi:HER2

MGGSPAGSPTSTEEGTSESATPESGPGTSTEPSEGSAPGSPAGSPTSTEEGTSTEPSEGSAPGTSTEPSEGSAPG
TSESATPESGPGSEPATSGSETPGSEPATSGSETPGSPAGSPTSTEEGTSESATPESGPGTSTEPSEGSAPGTST
EPSEGSAPGSPAGSPTSTEEGTSTEPSEGSAPGTSTEPSEGSAPGTSESATPESGPGTSTEPSEGSAPGTSESAT
PESGPGSEPATSGSETPGTSTEPSEGSAPGTSTEPSEGSAPGTSESATPESGPGTSESATPESGPGSPAGSPTST
EEGTSESATPESGPGSEPATSGSETPGTSESATPESGPGTSTEPSEGSAPGTSTEPSEGSAPGTSTEPSEGSAPG
TSTEPSEGSAPGTSTEPSEGSAPGTSTEPSEGSAPGSPAGSPTSTEEGTSTEPSEGSAPGTSESATPESGPGSEP
ATSGSETPGTSESATPESGPGSEPATSGSETPGTSESATPESGPGTSTEPSEGSAPGTSESATPESGPGSPAGSP
TSTEEGSPAGSPTSTEEGSPAGSPTSTEEGTSESATPESGPGTSTEPSEGSAPSGSGTSESATPESGPGSEPATSG
GSETPGTSESATPESGPGSEPATSGSETPGTSESATPESGPGTSTEPSEGSAPGSPAGSPTSTEEGTSESATPES
GPGSEPATSGSETPGTSESATPESGPGSPAGSPTSTEEGSPAGSPTSTEEGTSTEPSEGSAPGTSESATPESGPG
TSESATPESGPGTSESATPESGPGSEPATSGSETPGSEPATSGSETPGSPAGSPTSTEEGTSTEPSEGSAPGTST
EPSEGSAPGSEPATSGSETPGTSESATPESGPGTSTEPSEGSAPSSSSGSSSSGGSMSGTREPMDLTNC DREPIH
QLGAIQPFGLLQVSSDWIVTRASVNLAEFLGVTQADALGRPASTLIMPEALHTIRNKLTTLRGADVVERVFAIA
LTPDQSKFDVAVHFNESQVIEGERCQEDRRNAPSLSMRSMMSRLDQAETLEAFFREGARQARALTGFDRVMVYR
FDEGGSGEVVAEAARSIGSFLGLHYPASDIPVQARALYLRNLFRIIADVDAVPVPI LPERDEHGQPLDLSMSVL
RSVSPIHIEYLKNNMGV GASLSISIVVDGKLWGLFACHHYEPRLPSAQSRSTAELFGQMFASRLSRERRLALDYE
TKARRIADRLT SVADNASLLDDPAWLEALADAI PADGIGVWINGRLALAGIGPDKKNFASLVRHLNRNAGGRI
YAVDRLSQTYPDLEIDAVVAGMLAIPISRSRPRDYVVLFRQELVRTVVRWGGDPHKPVEYGPNGPRLTPRKSFEWS
ELVRGRSLPFTEAEQ RVAETIRVTLIEVVLRLTDEASMARQMANERQELLIAELN SSSSGSSSSGEQKLI SEEDV
DNKFNKEMRNAYWEIALLPNLNNQOKRAFRSLYDDPSQSANLLAEAKKLNDQAQPKHHHHHHHHH

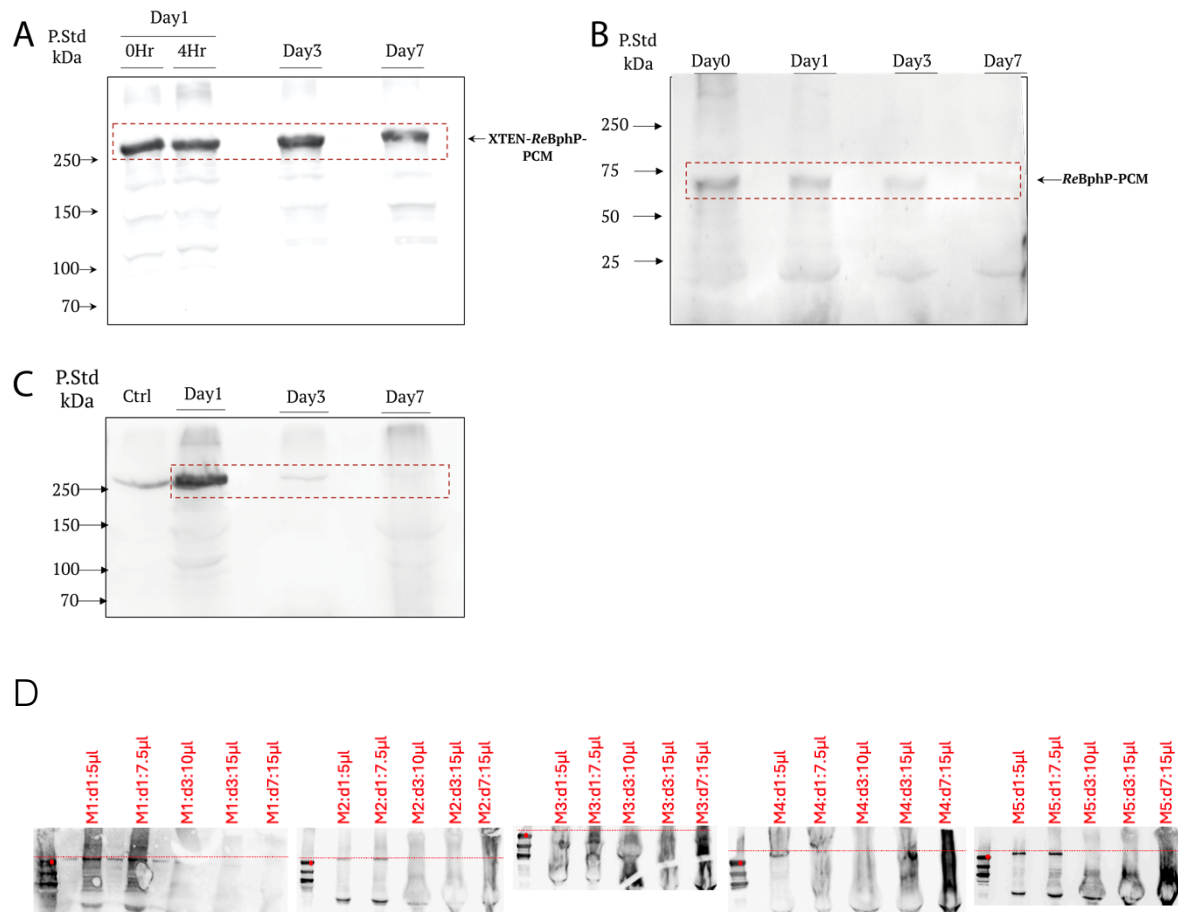
Supplemental Figure 1: Sequence of XTEN-ReBphP-PCM and XTEN-ReBphP-PCM-Affi:HER2. Residues are colored as XTEN (gray), linker (cyan), ReBphP-PCM (red), Affi:Her2¹ (green) and purification 8 x histidine tag (yellow).



Supplemental Figure 2: Exemplary purification procedure confirmation for XTEN-ReBphP-PCM. Representative chromatograms for the consecutive purification steps of XTEN-ReBphP-PCM: **a** metal affinity purification (IMAC), **b** Ion Exchange; and **c** Size Exclusion Chromatography (SEC). The fractions of the flow profile that were pooled and carried over to the next purification step are marked in blue. For the pooled fractions from the last purification step (**c**, SEC) a Coomassie stained SDS-PAGE (7% Acrylamide) is shown (**d**). **e** Storage conditions of the lyophilized protein at room temperature (RT) and -20°C. Proteins was measured after purification (day 0), lyophilized, and stored for the indicated time at the given temperature. The protein was resuspended and measured. Photoswitching between Pr (induced with 770 nm illumination) and Pfr (induced with 680 nm illumination) is shown as a confirmation of functionality.



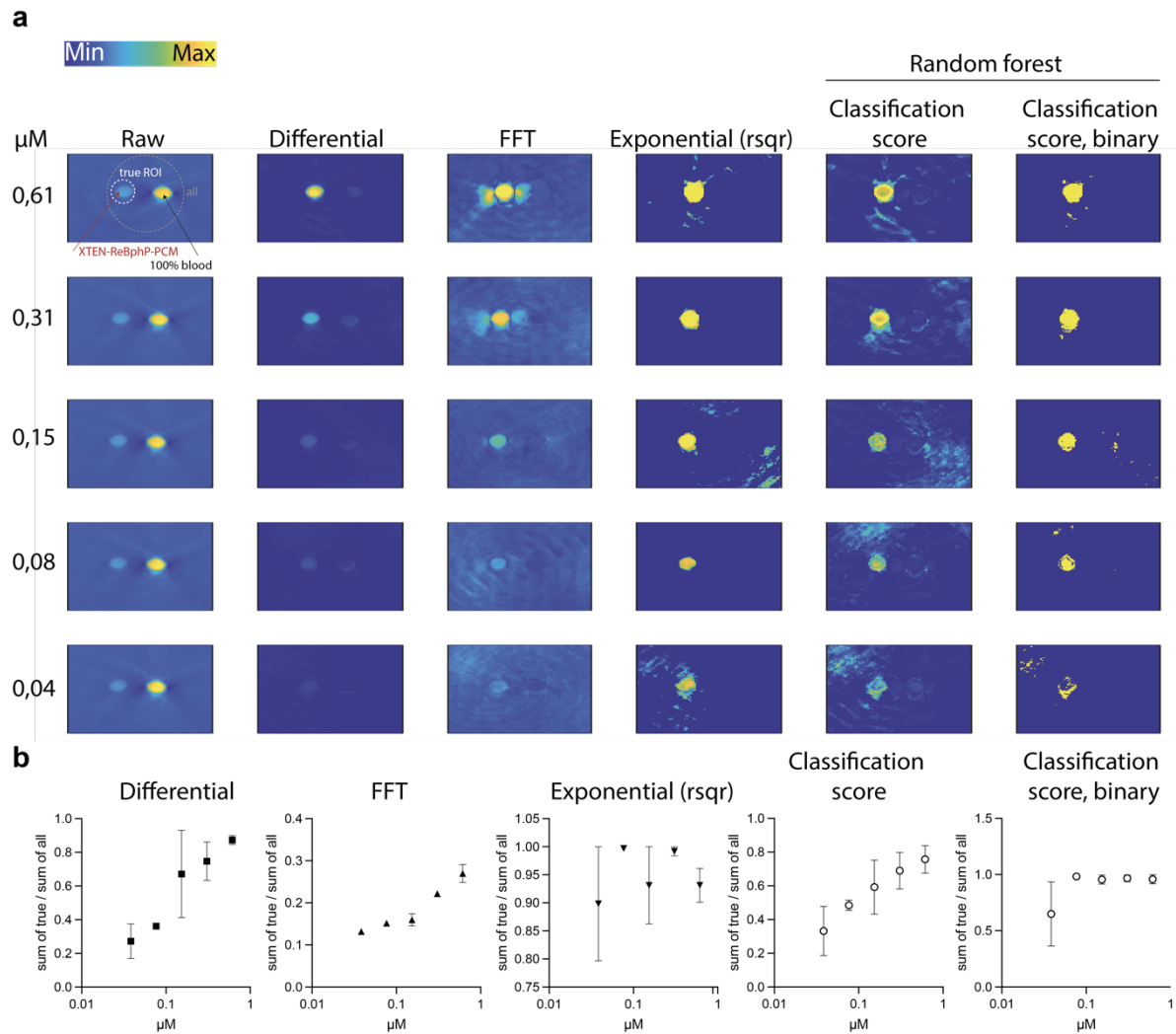
Supplemental Figure 3: Full spectra of XTEN-*ReBphP*-PCM, XTEN-*ReBphP*-PCM-Affi and parent *ReBphP*-PCM. Representative spectra are normalized to the protein peak at 280 nm. The Soret bands show similar heights which is indicative of a similarly effective chromophorylation with the Biliverdin chromophore in both proteins despite the XTEN in XTEN-*ReBphP*-PCM. The small different can be attributed to the normalization to the protein peak and the slightly higher extinction coefficient for the protein peak for XTEN-*ReBphP*-PCM ($49515 \text{ M}^{-1} \text{ cm}^{-1}$) and even more for XTEN-*ReBphP*-PCM-Affi ($56505 \text{ M}^{-1} \text{ cm}^{-1}$) compared to *ReBphP*-PCM ($48025 \text{ M}^{-1} \text{ cm}^{-1}$).



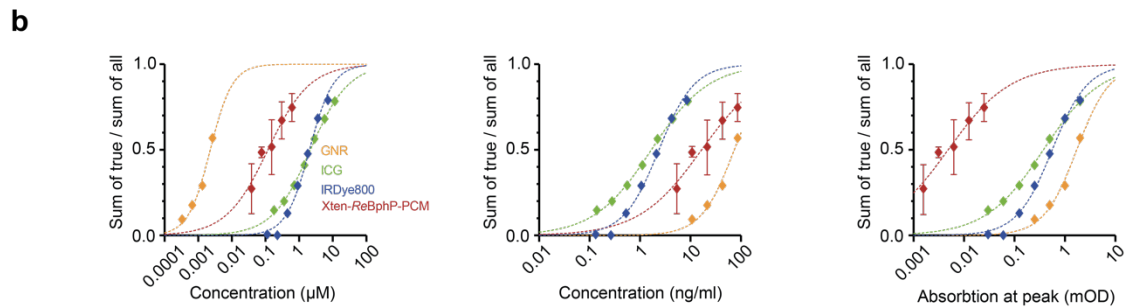
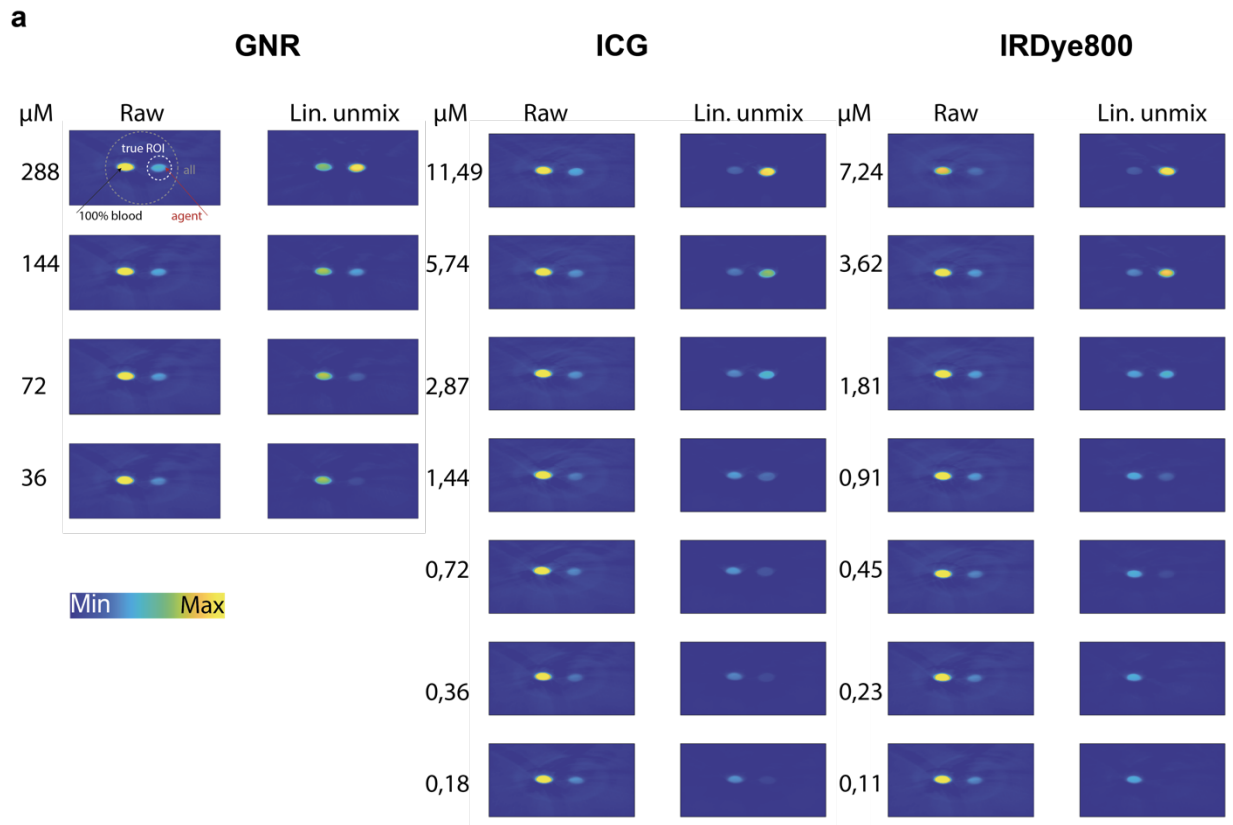
Supplemental Figure 4: *In vitro* and *in vivo* stability of XTEN-ReBphP-PCM. (a) & (b) Incubation of XTEN-ReBphP-PCM and ReBphP-PCM at 37°C in 50% mice plasma respectively and analyzed at Day 1, 3 & 7 **(c)** 0.75 mg of XTEN-ReBphP-PCM was injected into a C57BL/6 mice and pooled blood samples (N=5) were analyzed at Day 1, 3 and 7, along with the purified XTEN-ReBphP-PCM as positive control. Samples were analyzed by western blot and detected with anti-penta-HisTag antibody. 7% SDS PAGE **(a & c)**; 10% SDS PAGE **(b)**; Primary antibody: mouse anti-penta HisTag; Secondary antibody: goat anti-mouse HRP conjugated (1:10000). Red dotted rectangles show the expected band region. Shown are gel from one pooled sample per experimental condition. **(d)** Western blotting, as described in **(c)**, but conducted for individual plasma sample from each mouse. For quantitative analysis (Figure 1g), band intensity corrected by lane background and normalized by loaded volume was used. The loaded material for each sample was normalized to the respective protein concentration, which was determined via BCA assay for that mouse and time point. 250 kDa band is indicated by a red dot. Red line is located slightly above the presumed band height. Some lanes irregular migration patterns due to other proteins in plasma.

Supplemental Table 1: Optoacoustic measurements and unmixing concepts of studied samples and mice

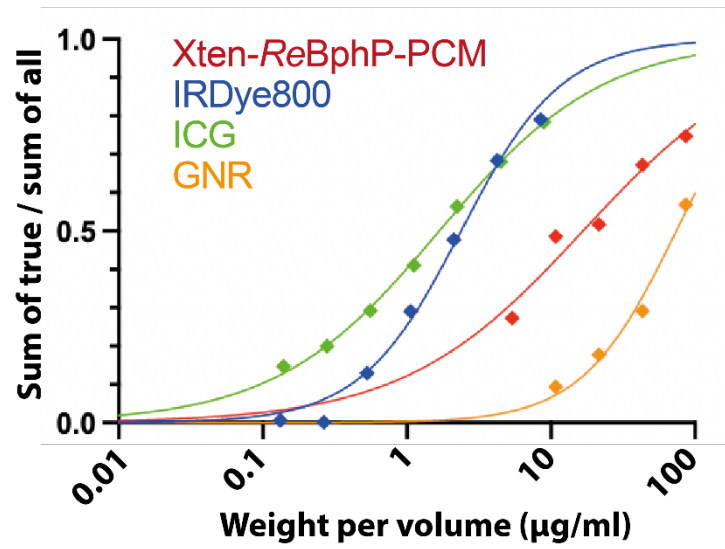
experiment	sample / mouse	agent	measurement characteristics	analysis characteristics	N	figure		
phantom comparison of purified XTEN-ReBHP-PCM and other agents	phantom 3% L, 2% LMA, 100% blood confounder 5 mm straw	purified XTEN-ReBHP-PCM 0.51; 0.31; 0.15; 0.08; 0.04 μM	(680 x 11 x 770 x 11) x 20	switching	N = 1	Fig. 2a and Suppl. Fig. 5 and 6		
		lipor R80x800 CW 7.24; 3.62; 1.81; 0.91; 0.45; 0.23; 0.11 μM	(680x5.960) x 10	lin unmixing (Hb, HbO, Lipid, H2O, IRdye800CW)	N = 1	Fig. 2a and Suppl. Fig. 5 and 6		
phantom comparison of HER2 targeting XTEN-ReBHP-PCM-Aff and R800-AB	phantom 1% L, 2% LMA, 100% blood confounder 580 μM catheter tubing	ICG	(680x5.960) x 10	lin unmixing (Hb, HbO, Lipid, H2O, ICG)	N = 1	Fig. 2a and Suppl. Fig. 5 and 6		
		11.49; 5.74; 2.87; 1.44; 0.72; 0.36; 0.18 μM	(680x5.960) x 10	lin unmixing (Hb, HbO, Lipid, H2O, 10 mm GNR)	N = 1	Fig. 2a and Suppl. Fig. 5 and 6		
		10 mm silica coated GNR	(11 x 680 x 11 x 770) x 50	switching	N = 1 of 3	Fig. 2b and Suppl. Fig. 8		
		0.0295; 0.0013; 0.0005; 0.0003; (0.0001) μM	(11 x 680 x 11 x 770) x 50	switching	N = 1 of 3	Fig. 2b and Suppl. Fig. 8		
		SKOV3 / XTEN-ReBHP-PCM-Aff 156,000; 82,100; 62,300; 47,700 cells/μl	(11 x 680 x 11 x 770) x 50	switching	N = 1 of 3	Fig. 2b and Suppl. Fig. 8		
		SKOV3 / XTEN-ReBHP-PCM-Aff 107,000; 72,000; 49,000; 33,000; 22,000; 16,000 cells/μl	(11 x 680 x 11 x 770) x 50	switching	N = 1 of 3	Fig. 2b and Suppl. Fig. 8		
		SKOV3 / XTEN-ReBHP-PCM-Aff 107,000; 72,000; 49,000; 33,000; 22,000; 16,000 cells/μl	(680x2.960) x 16	lin unmixing (Hb, HbO, Lipid, H2O, IRdye800CW)	N = 1 of 3	Fig. 2b and Suppl. Fig. 8		
		SKOV3 / R800-AB 172,000; 105,600; 75,000; 50,000; 33,000 cells/μl	(680x2.960) x 16	lin unmixing (Hb, HbO, Lipid, H2O, IRdye800CW)	N = 1 of 3	Fig. 2b and Suppl. Fig. 8		
		SKOV3 / R800-AB 105,000; 71,000; 47,000; 31,000 cells/μl	(680x2.960) x 16	lin unmixing (Hb, HbO, Lipid, H2O, IRdye800CW)	N = 1 of 3	Fig. 2b and Suppl. Fig. 8		
		SKOV3 / R800-AB 105,000; 71,000; 47,000; 31,000 cells/μl	(680x2.960) x 16	lin unmixing (Hb, HbO, Lipid, H2O, IRdye800CW)	N = 1 of 3	Fig. 2b and Suppl. Fig. 8		
Ex vivo mouse comparison of HER2 targeting XTEN-ReBHP-PCM-Aff and R800-AB	ex vivo FoxN1 nude dorsal <u>left</u>	SKOV3 / XTEN-ReBHP-PCM-Aff 156,000; 82,100; 62,300; 47,700 cells/μl	(11 x 680 x 11 x 770) x 50	switching	N = 1 of 3	Fig. 2c and Suppl. Fig. 9		
		SKOV3 / XTEN-ReBHP-PCM-Aff 72,000; 49,000; 33,000; 22,000; 16,000 cells/μl	(11 x 680 x 11 x 770) x 50	switching	N = 1 of 3	Fig. 2c and Suppl. Fig. 9		
		SKOV3 / XTEN-ReBHP-PCM-Aff 72,000; 49,000; 33,000; 22,000; 16,000 cells/μl	(11 x 680 x 11 x 770) x 50	switching	N = 1 of 3	Fig. 2c and Suppl. Fig. 9		
		SKOV3 / R800-AB 172,000; 105,600; 75,000; 50,000 cells/μl	(680x2.960) x 16	lin unmixing (Hb, HbO, Lipid, H2O, IRdye800CW)	N = 1 of 3	Fig. 2c and Suppl. Fig. 9		
		SKOV3 / R800-AB 105,000; 71,000; 47,000; 31,000 cells/μl	(680x2.960) x 16	lin unmixing (Hb, HbO, Lipid, H2O, IRdye800CW)	N = 1 of 3	Fig. 2c and Suppl. Fig. 9		
		SKOV3 / R800-AB 105,000; 71,000; 47,000; 31,000 cells/μl	(680x2.960) x 16	lin unmixing (Hb, HbO, Lipid, H2O, IRdye800CW)	N = 1 of 3	Fig. 2c and Suppl. Fig. 9		
		4T1 bearing mice injected with 0.75 mg of XTEN-ReBHP-PCM	FoxN1 nude 4T1 s.c. dorsal	0.75 mg XTEN-ReBHP-PCM i.v.	(11 x 680 x 11 x 770) x 50	switching	N = 1 of 3	Fig. 2d and Suppl. Fig. 21
				0.75 mg XTEN-ReBHP-PCM i.v.	(11 x 680 x 11 x 770) x 50	switching	N = 1 of 3	Fig. 2d and Suppl. Fig. 21
				0.75 mg XTEN-ReBHP-PCM i.v.	(11 x 680 x 11 x 770) x 50	switching	N = 1 of 3	Fig. 2d and Suppl. Fig. 21
				0.75 mg XTEN-ReBHP-PCM i.v.	(11 x 680 x 11 x 770) x 50	switching	N = 1 of 2	Suppl. Fig. 24
1.5 mg XTEN-ReBHP-PCM i.v.	(11 x 680 x 11 x 770) x 50			switching	N = 1 of 2	Suppl. Fig. 24		
0.75 mg XTEN-ReBHP-PCM i.v.	(11 x 680 x 11 x 770) x 50			switching	N = 1 of 2	Suppl. Fig. 25		
0.75 mg XTEN-ReBHP-PCM-Aff i.v.	(11 x 680 x 11 x 770) x 50			switching	N = 1 of 2	Suppl. Fig. 26		
0.75 mg XTEN-ReBHP-PCM-Aff i.v.	(11 x 680 x 11 x 770) x 50			switching	N = 1 of 4	Suppl. Fig. 26		
0.75 mg XTEN-ReBHP-PCM-Aff i.v.	(11 x 680 x 11 x 770) x 50			switching	N = 1 of 4	Suppl. Fig. 26		
0.75 mg XTEN-ReBHP-PCM-Aff i.v.	(11 x 680 x 11 x 770) x 50			switching	N = 1 of 4	Suppl. Fig. 26		
HCC1954 bearing mice injected with 0.75 mg of XTEN-ReBHP-PCM	FoxN1 nude SKOV3 s.c. dorsal	0.75 mg XTEN-ReBHP-PCM i.v.	(11 x 680 x 11 x 770) x 50	switching	N = 1 of 4	Fig. 2e and Suppl. Fig. 27		
		0.75 mg XTEN-ReBHP-PCM i.v.	(11 x 680 x 11 x 770) x 50	switching	N = 1 of 4	Fig. 2e and Suppl. Fig. 27		
		0.75 mg XTEN-ReBHP-PCM i.v.	(11 x 680 x 11 x 770) x 50	switching	N = 1 of 4	Fig. 2e and Suppl. Fig. 27		
		1 mg XTEN-ReBHP-PCM-Aff i.v.	(11 x 680 x 11 x 770) x 50	switching	N = 1 of 4	Fig. 2e and Suppl. Fig. 27		
		1 mg XTEN-ReBHP-PCM-Aff i.v.	(11 x 680 x 11 x 770) x 50	switching	N = 1 of 4	Fig. 2e and Suppl. Fig. 27		
		1 mg XTEN-ReBHP-PCM-Aff i.v.	(11 x 680 x 11 x 770) x 50	switching	N = 1 of 4	Fig. 2e and Suppl. Fig. 27		
		0.75 mg XTEN-ReBHP-PCM i.v.	(11 x 680 x 11 x 770) x 50	switching	N = 1 of 4	Fig. 2e and Suppl. Fig. 27		
		0.75 mg XTEN-ReBHP-PCM i.v.	(11 x 680 x 11 x 770) x 50	switching	N = 1 of 1	Suppl. Fig. 22		
		Control mouse without tumor	FoxN1 nude 4T1	0.75 mg XTEN-ReBHP-PCM i.v.	(11 x 680 x 11 x 770) x 50	switching	N = 5	Suppl. Fig. 23
				PBS	(11 x 680 x 11 x 770) x 50	switching	N = 5	Suppl. Fig. 23
mice injected with 0.75 mg of XTEN-ReBHP-PCM	FoxN1 nude	0.75 mg XTEN-ReBHP-PCM i.v.	(11 x 680 x 11 x 770) x 50	switching	N = 5	Suppl. Fig. 23		
		PBS	(11 x 680 x 11 x 770) x 50	switching	N = 5	Suppl. Fig. 23		
Ex vivo mice with sub cutaneous tumors and intravenous injection of agent	Ex vivo FoxN1 nude dorsal <u>left</u>	0.75 mg XTEN-ReBHP-PCM i.v.	(11 x 680 x 11 x 770) x 50	switching	N = 1 of 3	Fig. 2d and Suppl. Fig. 21		
		0.75 mg XTEN-ReBHP-PCM i.v.	(11 x 680 x 11 x 770) x 50	switching	N = 1 of 3	Fig. 2d and Suppl. Fig. 21		
		0.75 mg XTEN-ReBHP-PCM i.v.	(11 x 680 x 11 x 770) x 50	switching	N = 1 of 2	Suppl. Fig. 24		
		0.75 mg XTEN-ReBHP-PCM i.v.	(11 x 680 x 11 x 770) x 50	switching	N = 1 of 2	Suppl. Fig. 24		
		1.5 mg XTEN-ReBHP-PCM i.v.	(11 x 680 x 11 x 770) x 50	switching	N = 1 of 2	Suppl. Fig. 25		
		0.75 mg XTEN-ReBHP-PCM i.v.	(11 x 680 x 11 x 770) x 50	switching	N = 1 of 2	Suppl. Fig. 26		
		0.75 mg XTEN-ReBHP-PCM-Aff i.v.	(11 x 680 x 11 x 770) x 50	switching	N = 1 of 4	Suppl. Fig. 26		
		0.75 mg XTEN-ReBHP-PCM-Aff i.v.	(11 x 680 x 11 x 770) x 50	switching	N = 1 of 4	Suppl. Fig. 26		
		0.75 mg XTEN-ReBHP-PCM-Aff i.v.	(11 x 680 x 11 x 770) x 50	switching	N = 1 of 4	Suppl. Fig. 26		
		0.75 mg XTEN-ReBHP-PCM-Aff i.v.	(11 x 680 x 11 x 770) x 50	switching	N = 1 of 4	Suppl. Fig. 26		
Excised Organs	Excised Organs	0.75 mg XTEN-ReBHP-PCM i.v.	(11 x 680 x 11 x 770) x 50	switching	N = 5	Suppl. Fig. 23		
		PBS	(11 x 680 x 11 x 770) x 50	switching	N = 5	Suppl. Fig. 23		



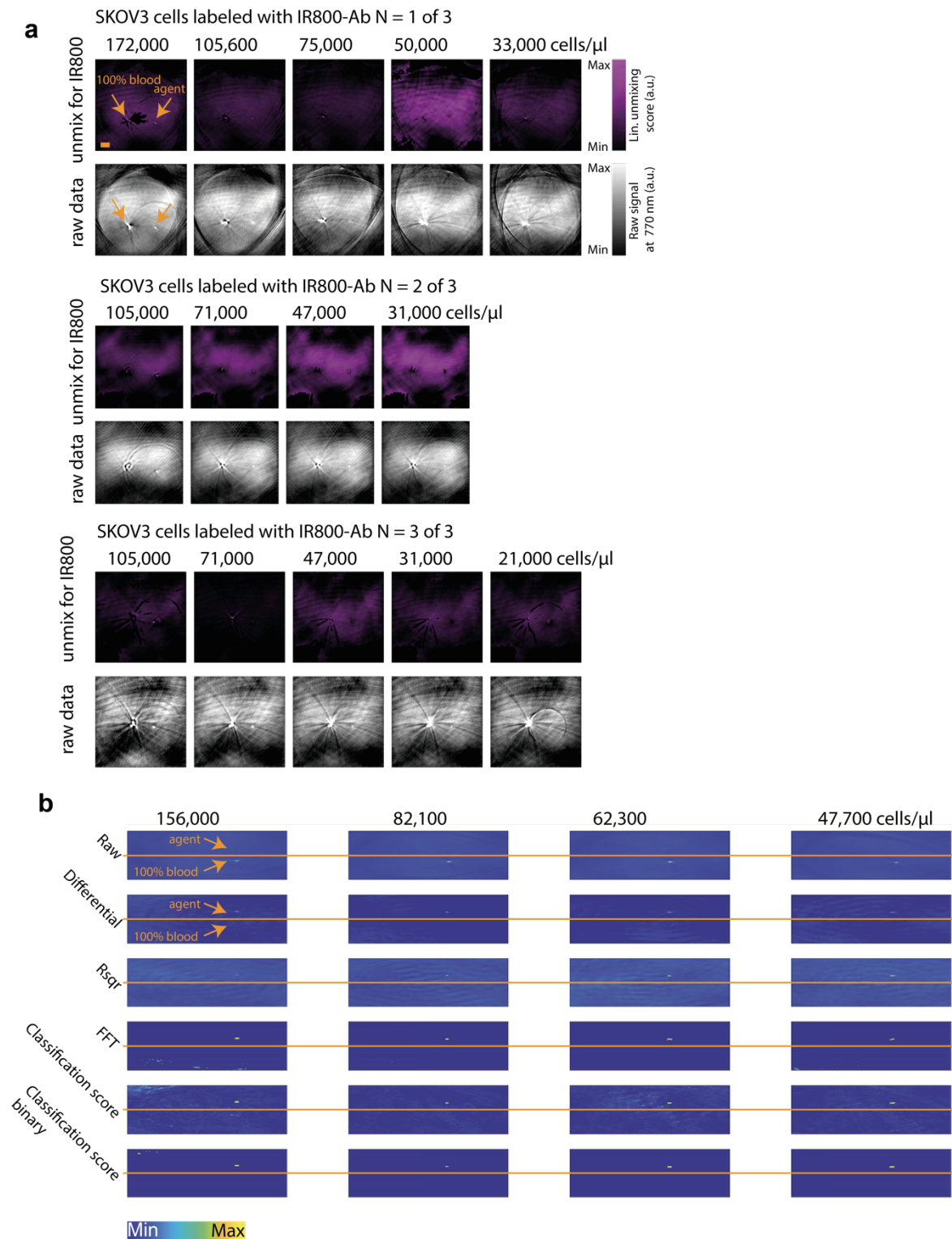
Supplemental Figure 5: Unmixed raw images of Phantom measurements for XTEN-ReBphP-PCM. Phantoms consists of two straws: one sample straw filled with full blood and the other with indicated concentration of XTEN-ReBphP-PCM. Both straws are embedded at the center of a tissue-mimicking phantom consisting of 2% Agarose & 3% IL. **a** Shown are representative slices for all concentrations as raw data (very left) and unmixed based on the different metrics (see methods for details). Numerical analysis was performed by dividing the sum of the pixel values in the “true roi” selection by the sum of pixel values in the “all” selection. This reflects the quality of unmixing very stringently but is strongly affected by even light background which gets emphasized by the sum over all pixels in the large region (as is the case in the FFT analysis). The “true roi” region was chosen larger; while this underestimates lower concentrations it compensates for the reconstruction inherent sidelobes seen for the unmixing in the high concentrations. A perfect unmixing with no background would hence yield 1 since the detected pixels in the “true roi” == the pixels in the “all” roi. This does not inform about the recall rate (i.e. true positives vs. expected positives) since the definition of the exact extent of the tubing signal (i.e. expected positives) is challenging. All images show the same colormap (top left) indicative of the respective metric of the given column and scaled to min/max for the complete column. **b** Shows the individual metrics for the numerical analysis. Shown is mean and standard deviation over three slices. The used exponential model allowed negative rsqr; to prevent confusion in assessing the sum values negative rsqr was set to zero. Similarly, a negative differential is possible but was similarly set to zero.



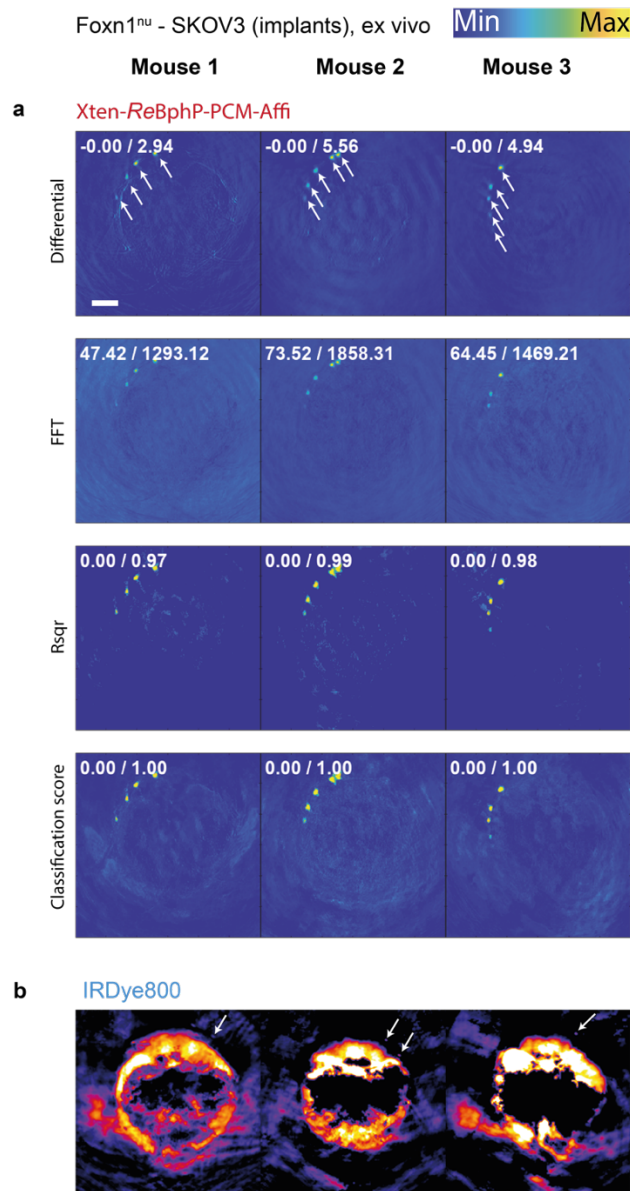
Supplemental Figure 6: a Unmixed raw images of Phantom measurements for GNR, ICG and IRDye800. Phantom and representation are like Suppl. Figure 4a. Linear unmixing was performed as described in the methods section. All images show the same colormap (bottom left) scaled to min/max for all samples of the given agent. **b Different representations of Figure 1h** shown based on mass concentration and absorption at peak.



Supplemental Figure 7: Sensitivity of unmixing of different agents represented as weight per volume. Similar data and graphic as in Figure 2a only represented in weight/volume

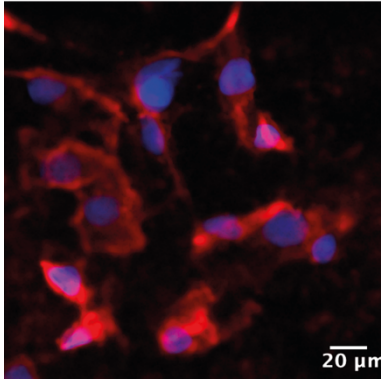


Supplemental Figure 8: Representative images of unmixing of different numbers of SKOV3 labeled with IR800-Ab (a) or ReBphp-PCM-Affi (b). In both cases agents are filled in 580 μ m catheter tubing and unmixed as described previously. Horizontal orange lines in b for orientation only. Colorbars in a show the linear unmixing score and the raw signal. Images are scaled min/max per row. The colorbar in b shows the respective metric with the images scaled min/max per row.

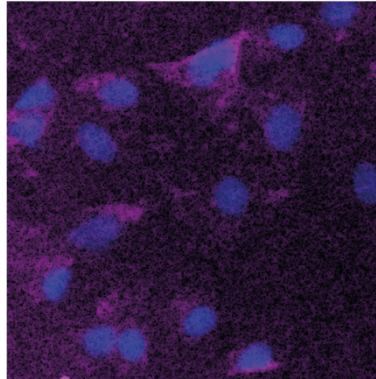


Supplemental Figure 9: Ex vivo mice with subcutaneous implants of SKOV3 cells labeled with XTEN-ReBphP-PCM-Affi or the non-photoswitchable agent IRDye800-AB (b). Shown are average intensity projections of 3 consecutive slices for 3 mice (columns). For XTEN-ReBphP-PCM-Affi (a) the metrics differential, FFT and exponential fit described by fit quality (rsqr) are shown together with the random forest classification approach combining the former three. To allow unbiased assessment all images are scaled between their maxima and minima (indicated at the left corner of each image) with the colorbar shown in the top right. Mouse 1 was implanted with, from top to bottom, (1) 156000 cells/ μ l, (2) 82100 cells/ μ l, (3) 62300 cells/ μ l, (4) 47700 cells/ μ l; mouse 2 and 3 with (1) 72000 cells/ μ l, (2) 49000 cells/ μ l, (3) 33000 cells/ μ l, (4) 22000 cells/ μ l, (5) 16000 cells/ μ l. Scale bar is 5 mm. For IRDye800-AB (b) the IRDye800 component after linear unmixing is shown. Images have been scaled to allow visualization of some of the tubes (indicated by arrows). Mouse 1 was implanted with, from top to bottom, (1) 172000 cells/ μ l, (2) 105600 cells/ μ l, (3) 75000 cells/ μ l, (4) 50000 cells/ μ l; mouse 2 and 3 with (1) 105000 cells/ μ l, (2) 71000 cells/ μ l, (3) 47000 cells/ μ l, (4) 31000 cells/ μ l. Arrows are only shown if implant could be clearly delineated in unmixing.

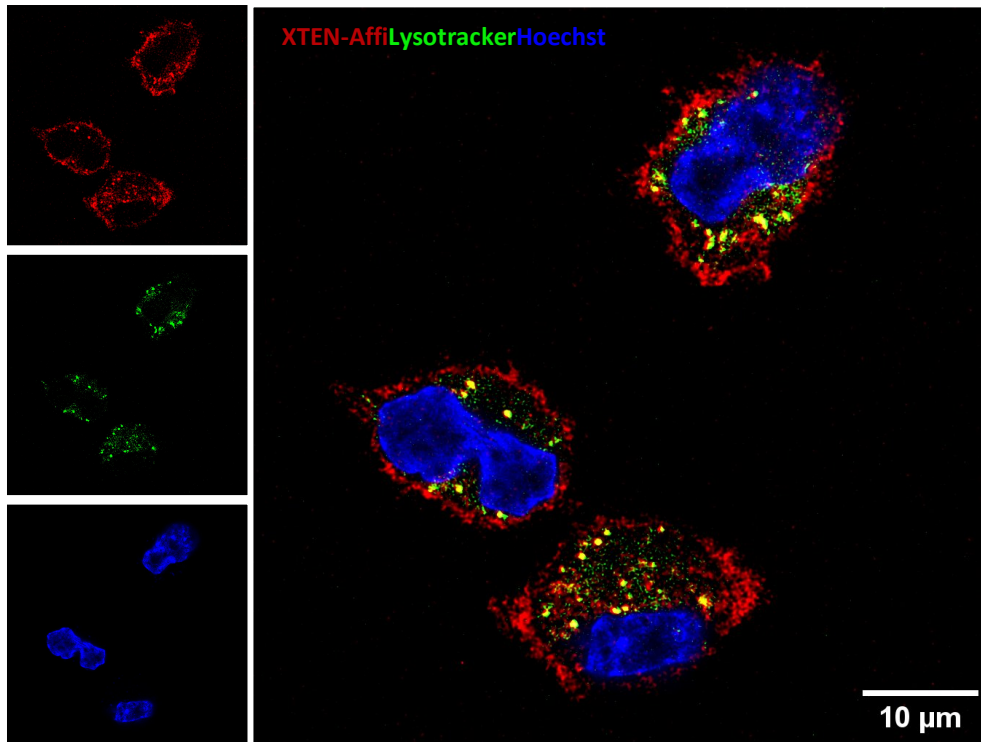
SKOV3 HER2-IR800-AB
Hoechst
IR



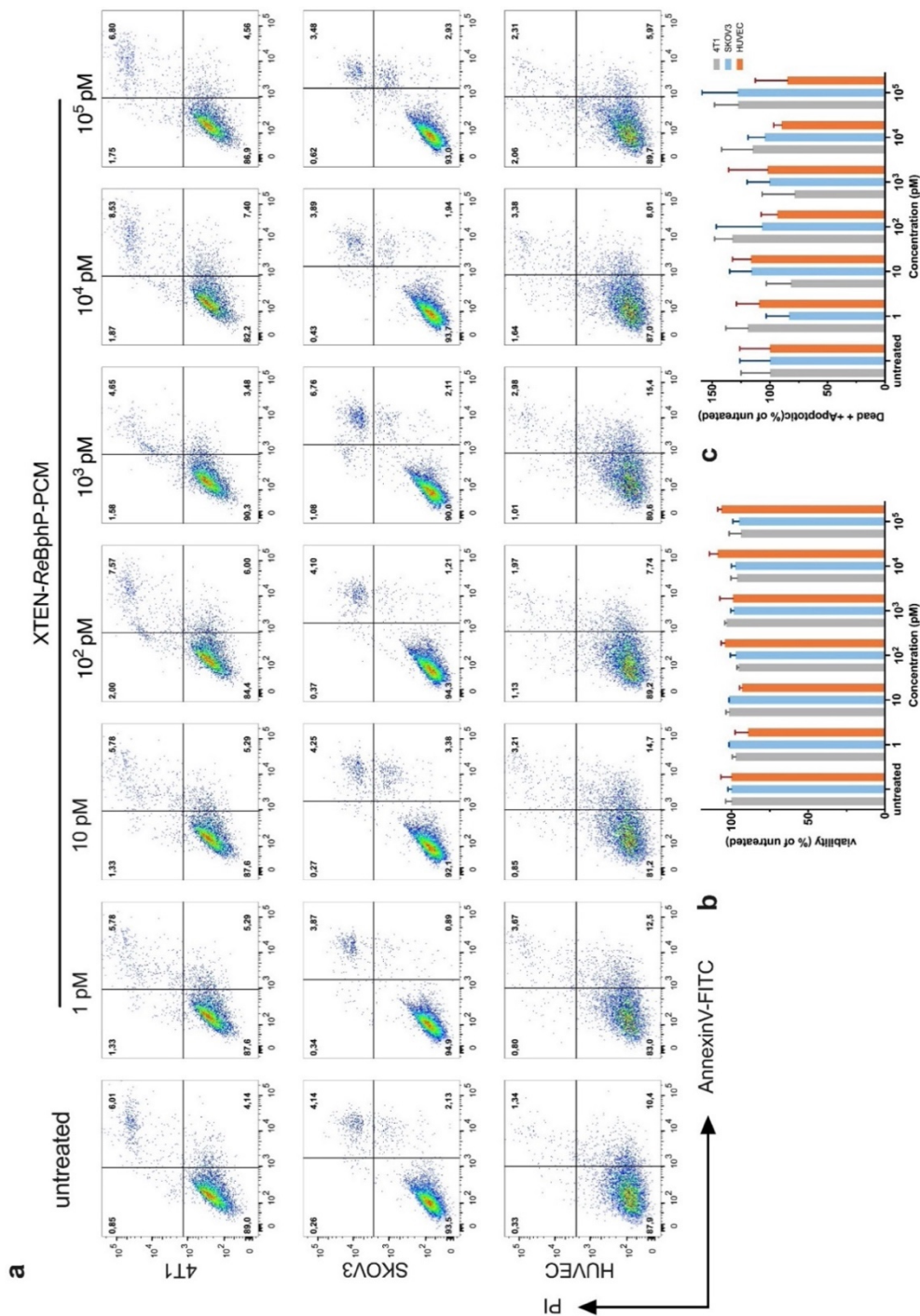
SKOV3 ReBphP-XTEN-Affi
Hoechst
Cy5



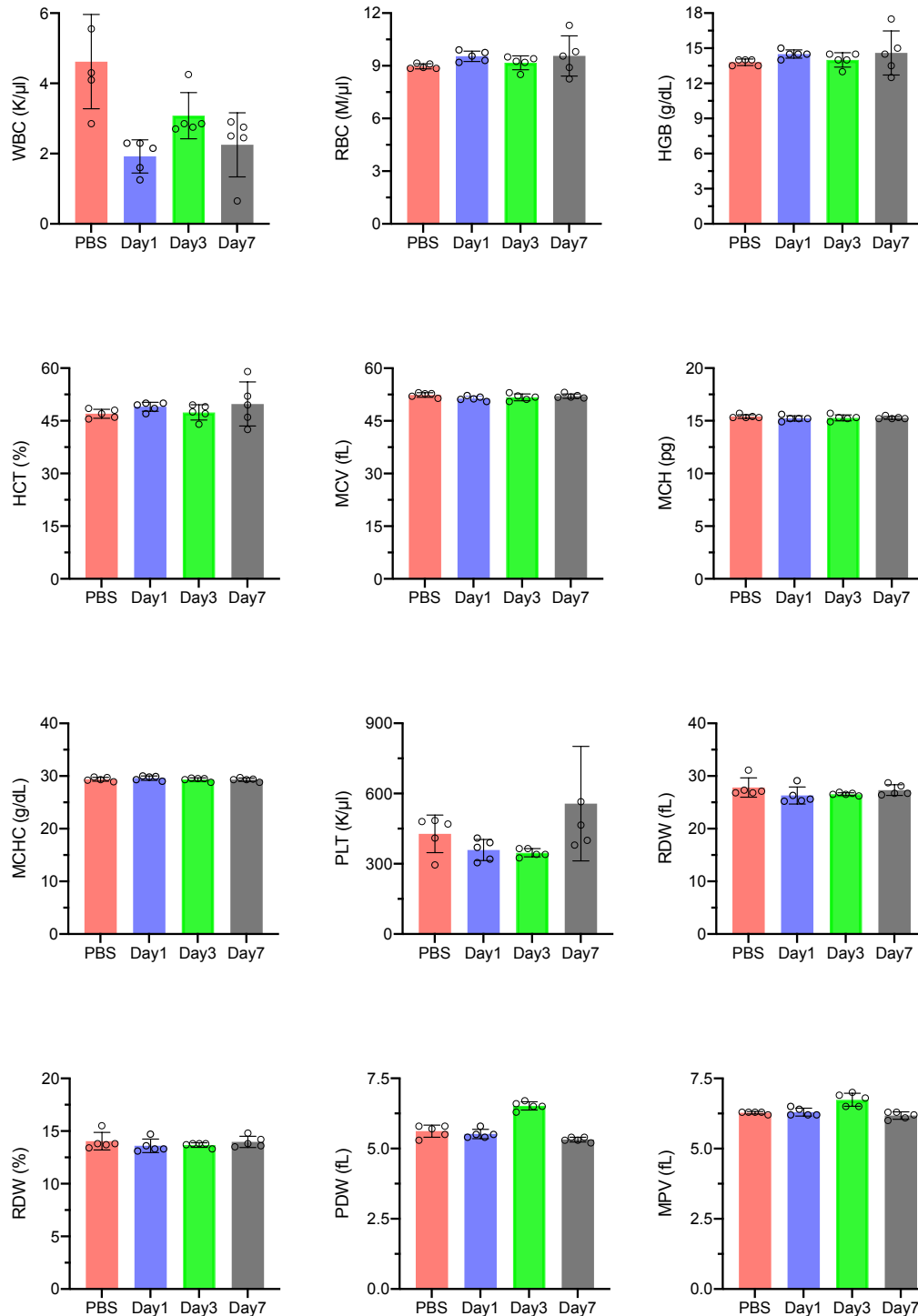
Supplemental Figure 10: Confocal images of SKOV3 labeled with XTEN-ReBphP-PCM-Affi (right) and IRDye800-AB (left). Excitation at 725 nm (IR channel) for IR800 and 633 nm (Cy5) for the residual fluorescence of ReBphP-PCM.



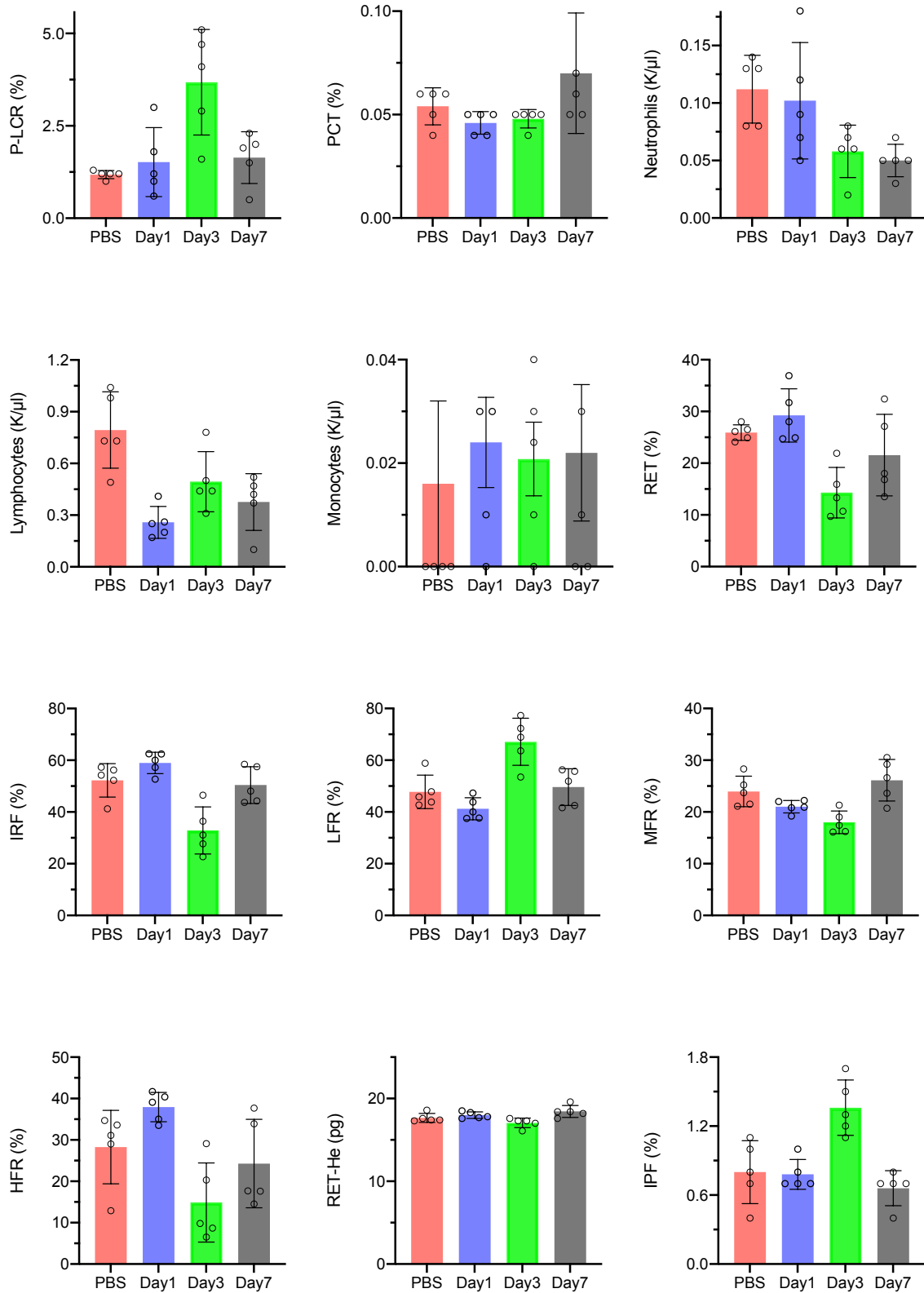
Supplemental Figure 11: Confocal images of SKOV3 stained with XTEN-*ReBphP*-PCM-Affi and LysoTracker. Excitation at 353 nm (Hoechst), 504 nm (lysosome) and 660 nm (Cy5.5) for the residual fluorescence of *ReBphP*-PCM. SKOV3 cells were incubated with XTEN-*ReBphP*-PCM-Affi for 3 hours and LysoTracker-Green DND-26 was added for the final hour of incubation.



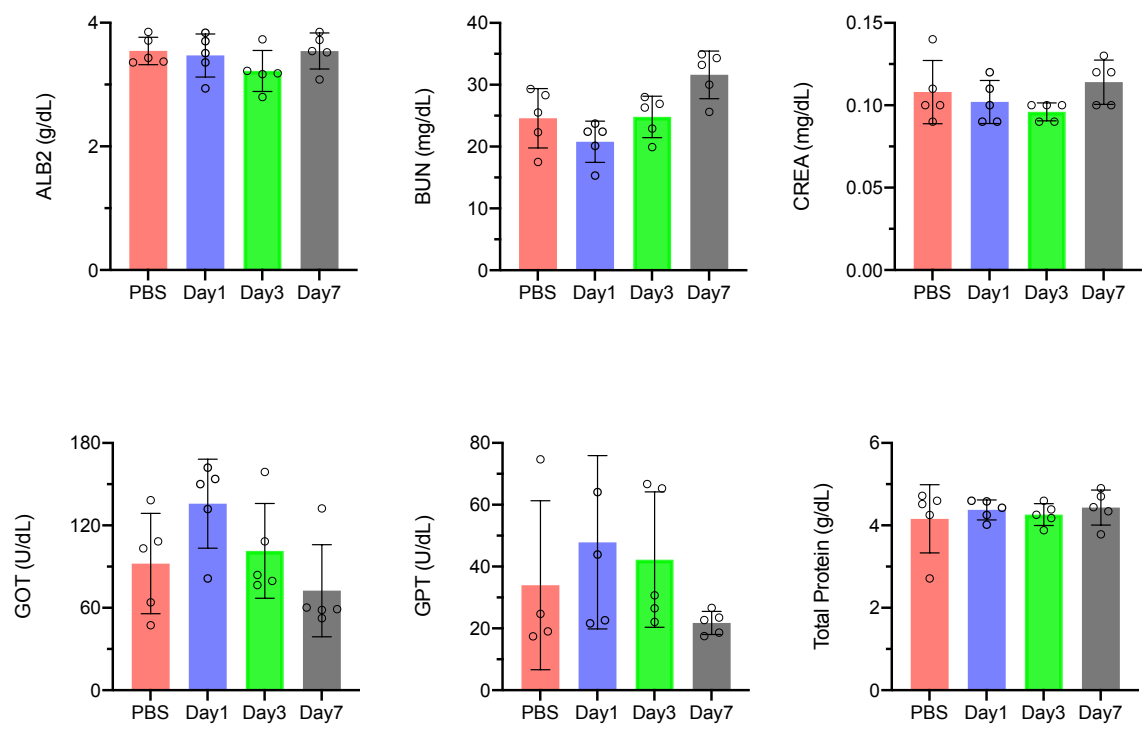
Supplemental Figure 12: Analysis by flow cytometry of 4T1, SKOV3 and HUVEC cell viability and apoptosis following treatment with XTEN-ReBphP-PCM. Cells were treated with XTEN-ReBphP-PCM at concentrations from 1 to 10⁵ pM for 72h, with triplicates, and labeled with Annexin V and Propidium iodide (PI) prior to analysis with flow cytometry. Concentration is chosen according to standard procedures². Shown are (a) Flow cytometric analysis results of cells treated with different concentrations of XTEN-ReBphP-PCM; (b) and (c) quantitative analysis of viabilities and percentages of dead and apoptotic cells normalized to the untreated respective levels. Living cells included the Annexin V⁻/PI⁻ cells, Apoptotic cells: Annexin V⁺/PI⁻, and dead cells: Annexin V⁺/PI⁺. Results are presented as means ± SD. *P<0.05.



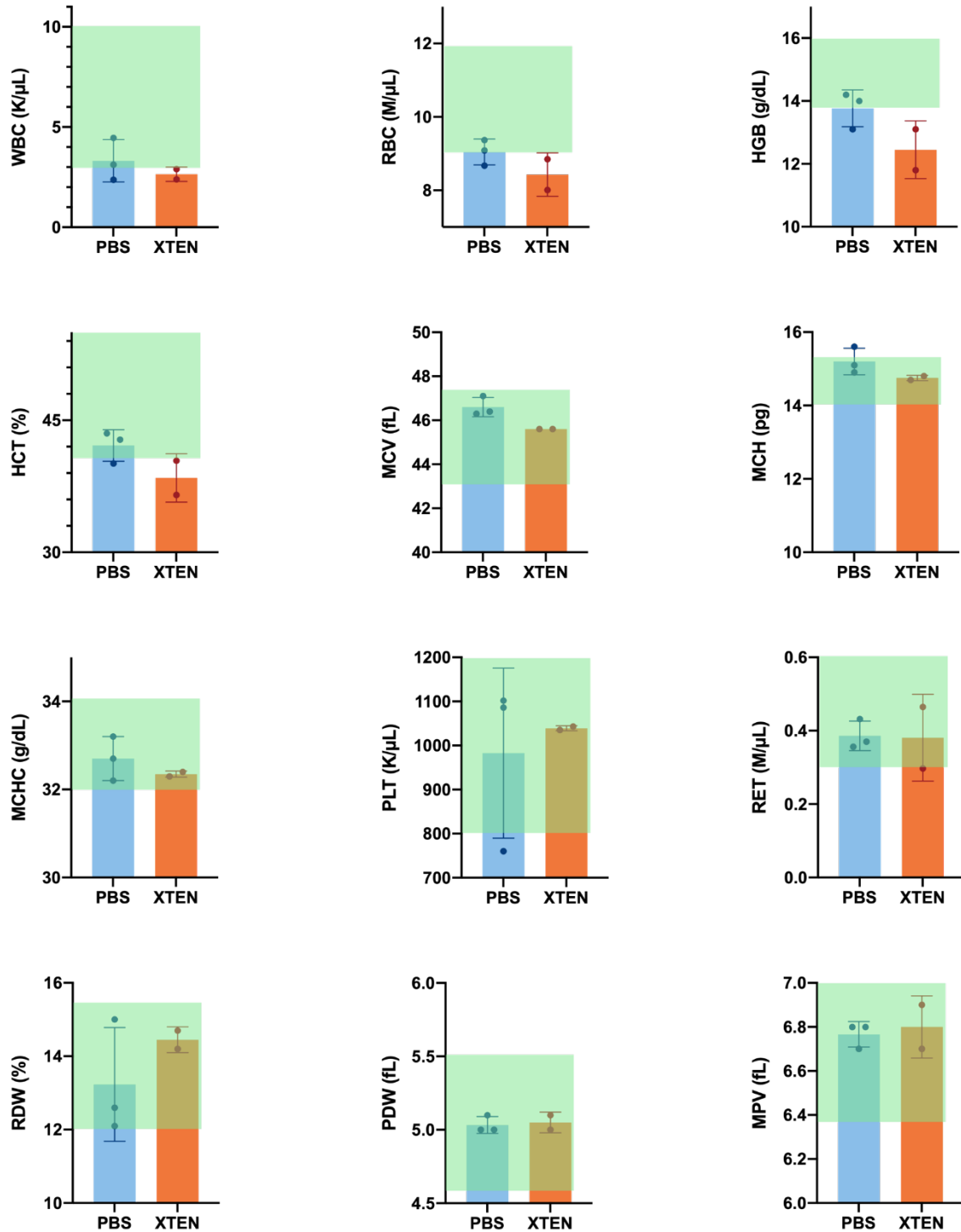
Supplemental Figure 13: Complete blood count analysis of C57BL/6 mice injected with XTEN-ReBphP-PCM. For each group n=4 mice were used, shown are the data points together with SD. The control group was injected *iv.* with PBS while all sample groups have been injected *iv.* with 750 μ g of XTEN-ReBphP-PCM and sacrificed after 4 h, 3 d or 7 d. Abbreviations: WBC = white blood cells, RBC = red blood cells, HGB = hemoglobin, HCT = hematocrit, MCV = mean corpuscular volume, MCH = mean corpuscular hemoglobin, MCHC = mean corpuscular hemoglobin concentration, PLT = platelet blood count, RDW = red cell distribution width PDW = platelet distribution width, MPV = mean platelet volume



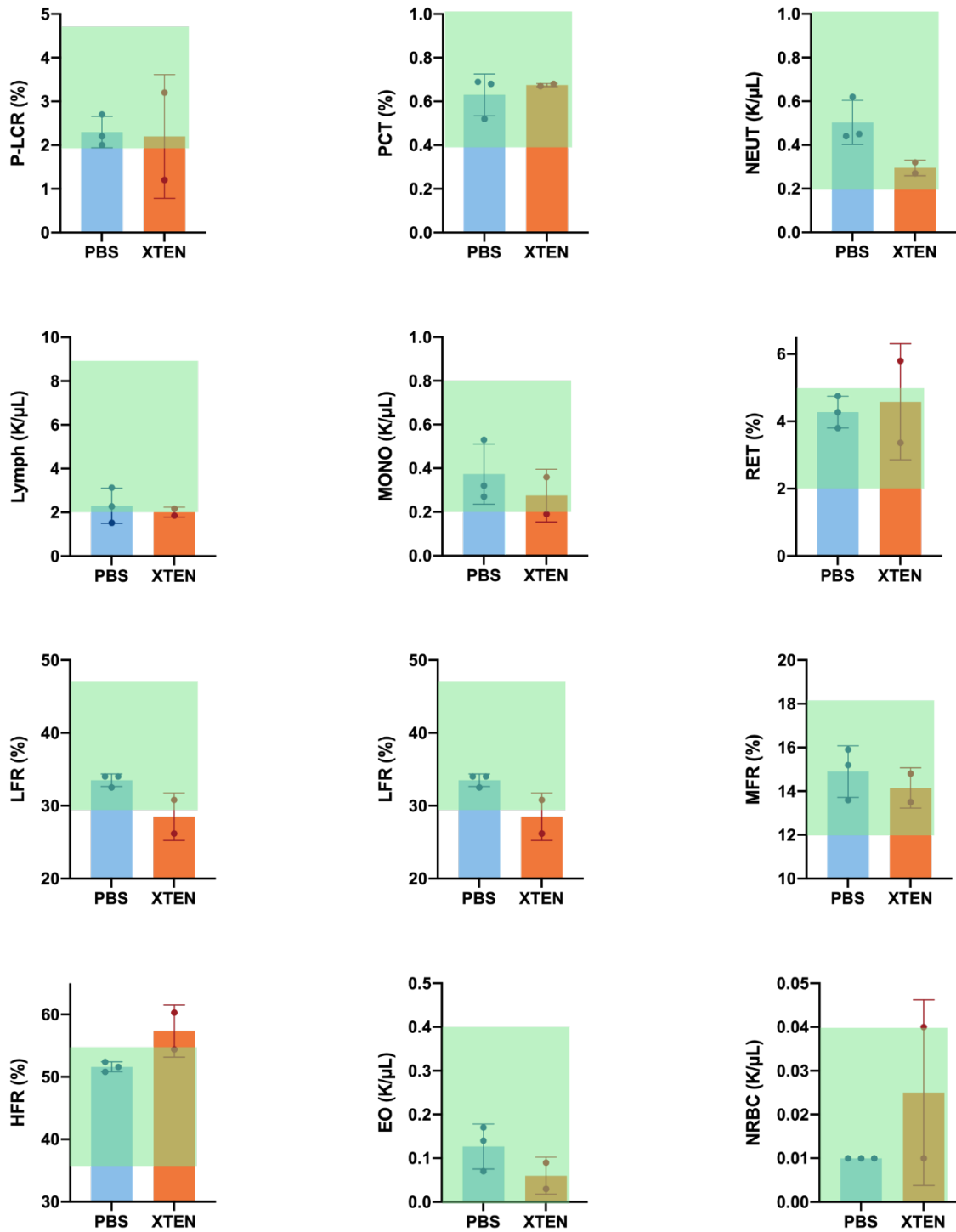
Supplemental Figure 14: Continuation of complete blood count analysis of C57BL/6 mice injected with XTEN-ReBphP-PCM. Abbreviations: P-LCR = platelet large cell ratio, PCT = procalcitonin, RET = reticulocytes, IRF = immature reticulocyte fraction, LFR = low fluorescence ratio, MFR = myocardial flow reserve, HFR = high fluorescence ratio, RET-He = reticulocyte hemoglobin equivalent, IPF = immature platelet fraction



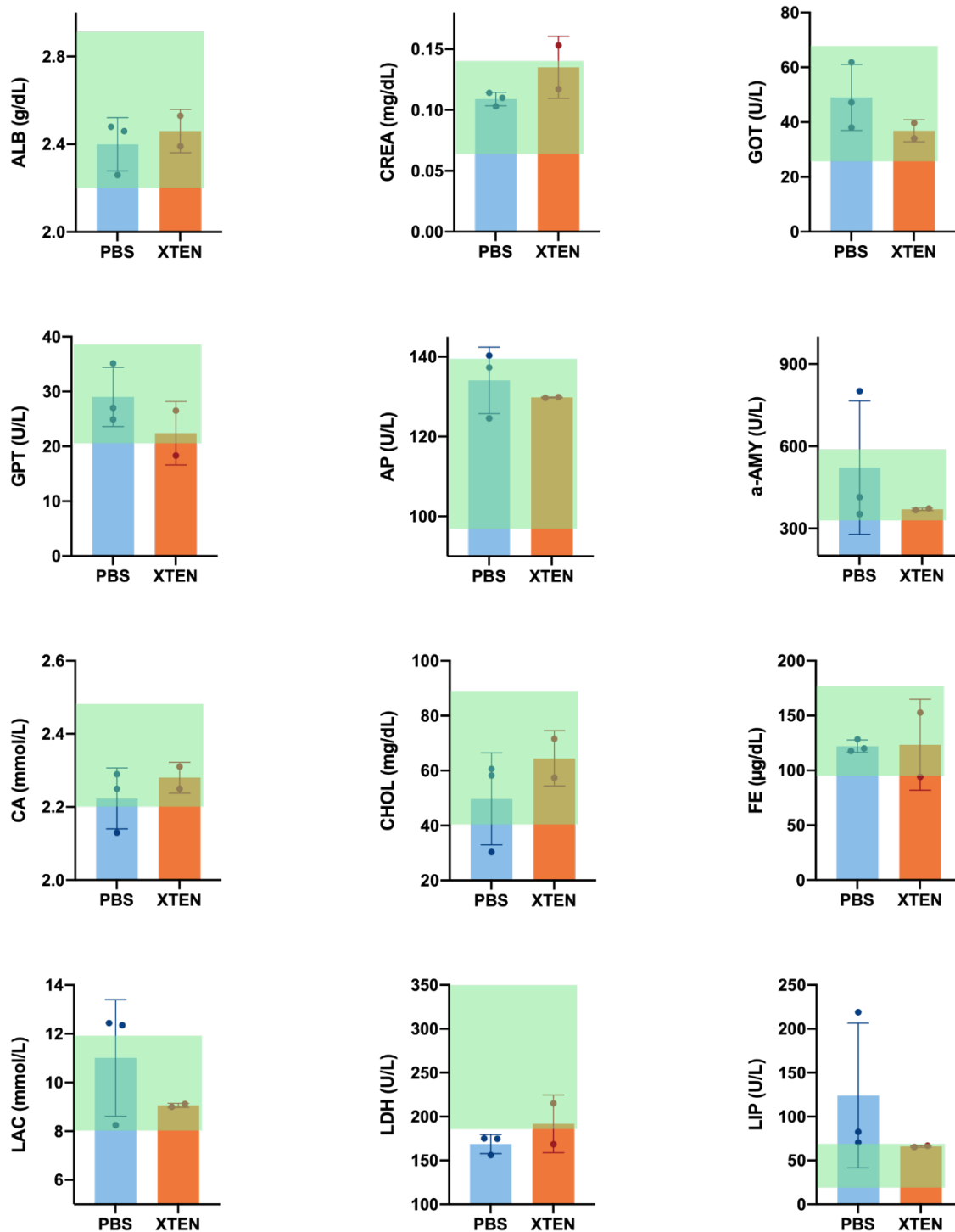
Supplemental Figure 15: Clinical chemistry testing results of C57BL/6 mice injected with XTEN-ReBphP-PCM. Abbreviations: ALB2 = albumin, BUN = blood urea nitrogen, CREA = creatine, GOT = glutamic-oxaloacetic transaminase, GPT = glutamic pyruvic transaminase.



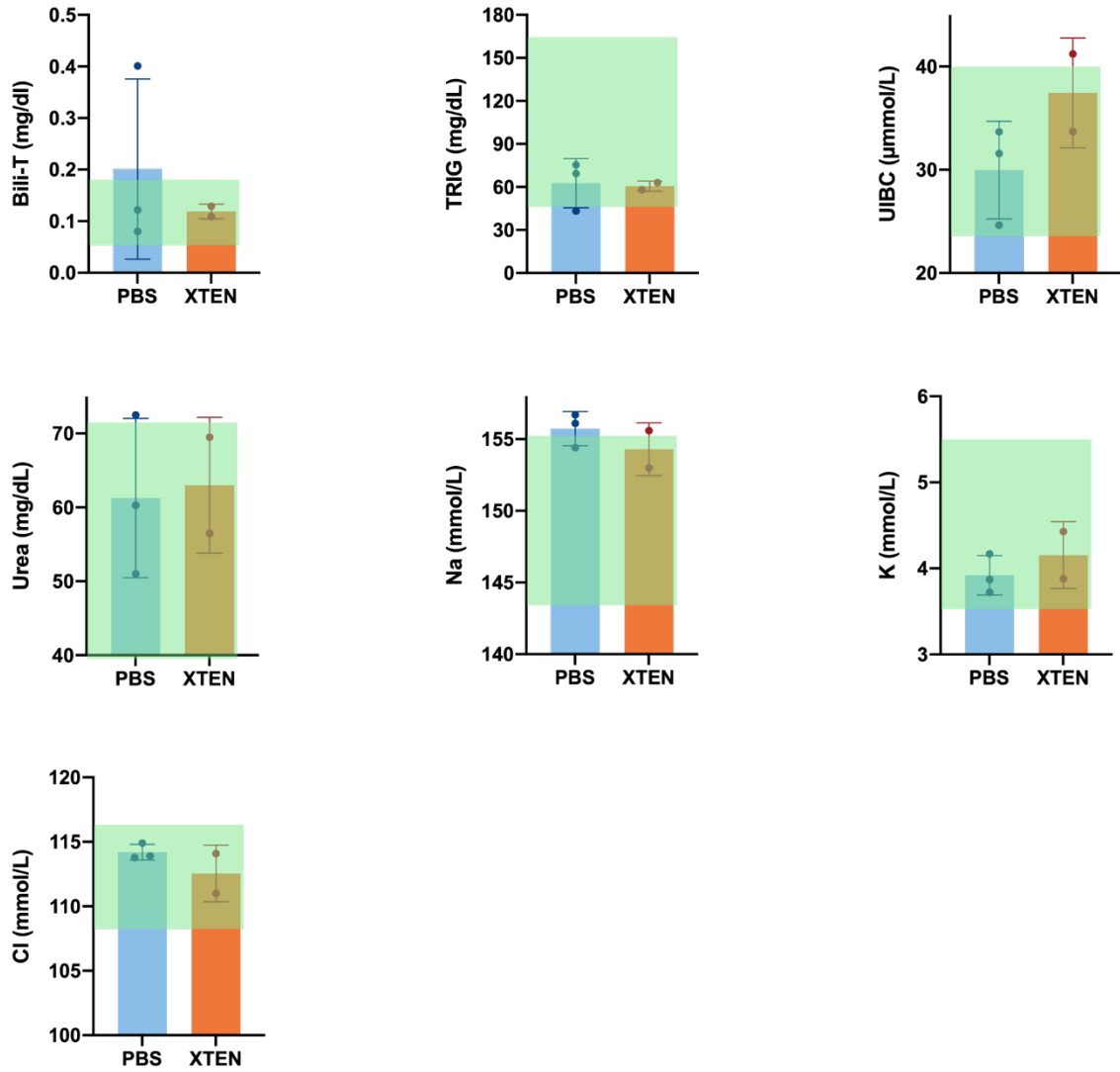
Supplementary Figure 16: Complete blood count analysis of C57BL/6 mice following weekly injections with XTEN-ReBphP-PCM. Mice were administered 750 μg XTEN-ReBphP-PCM (n=3) or PBS (control, n=3) for 3 weeks. Blood samples were collected 9 days after the final injection. Blood parameters were measured from EDTA-collected samples using a full blood count analysis. Normal ranges are marked in green. Values are presented as mean ± SD.



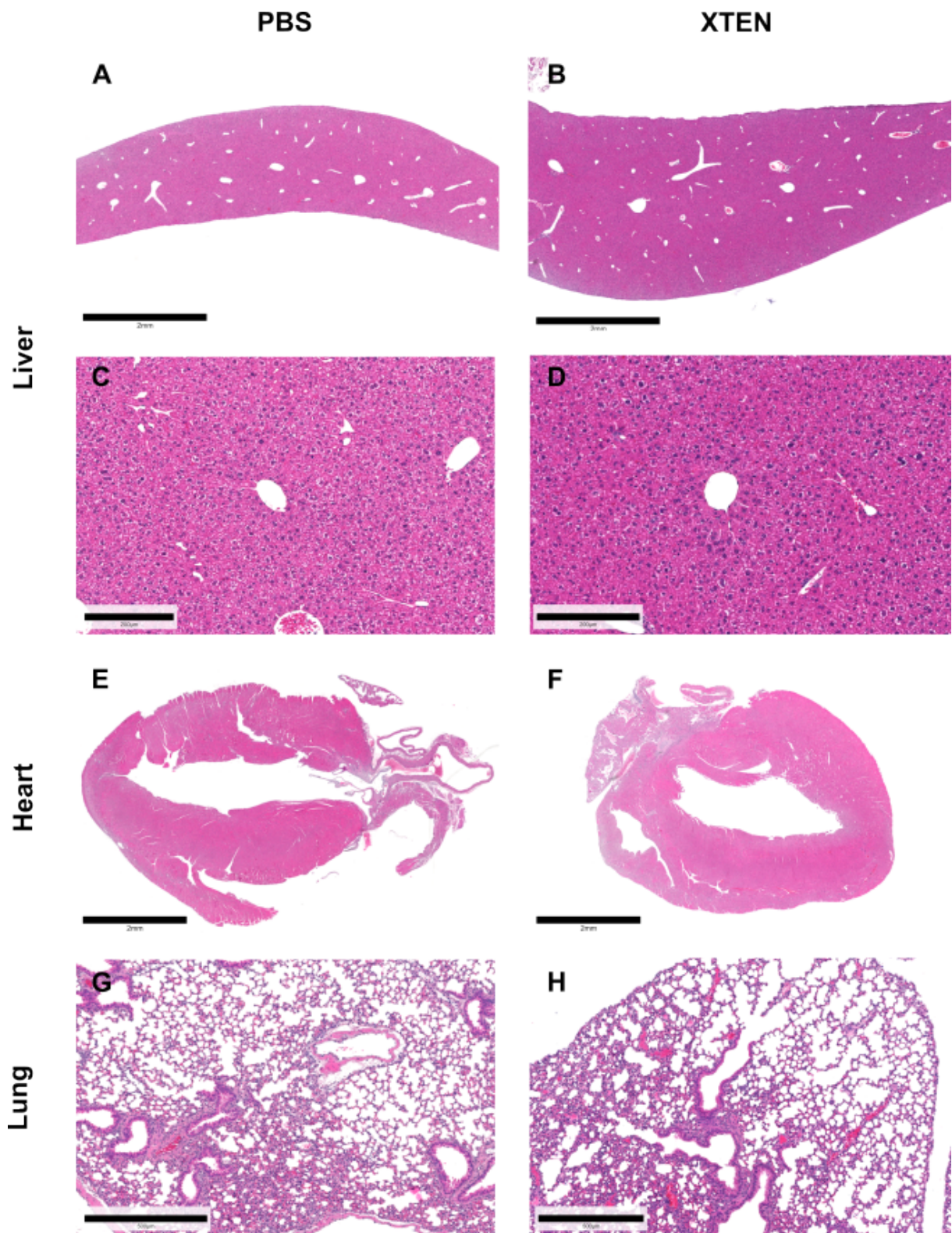
Supplementary Figure 17: Continuation of complete blood count analysis of C57BL/6 mice following weekly injections with XTEN-ReBphP-PCM. Abbreviations: EO = eosinophilic granulocyte, NRBC = nucleated red blood cell.



Supplementary Figure 18: Clinical chemistry testing results of C57BL/6 mice injected weekly with XTEN-ReBphP-PCM. Mice were administered with 750 µg XTEN-ReBphP-PCM (n=3) or PBS (control, n=3) for 3 weeks. Blood samples were collected 9 days after the final injection. Blood parameters were measured from plasma. Abbreviations: AP = alkaline phosphatase, a-AMY = alpha-amylase, CA = calcium, CHOL = total cholesterol, FE = iron, LAC = lactate, LDH = lactate dehydrogenase, LIP = lipase. Normal ranges are marked in green. Values are presented as mean ± SD.

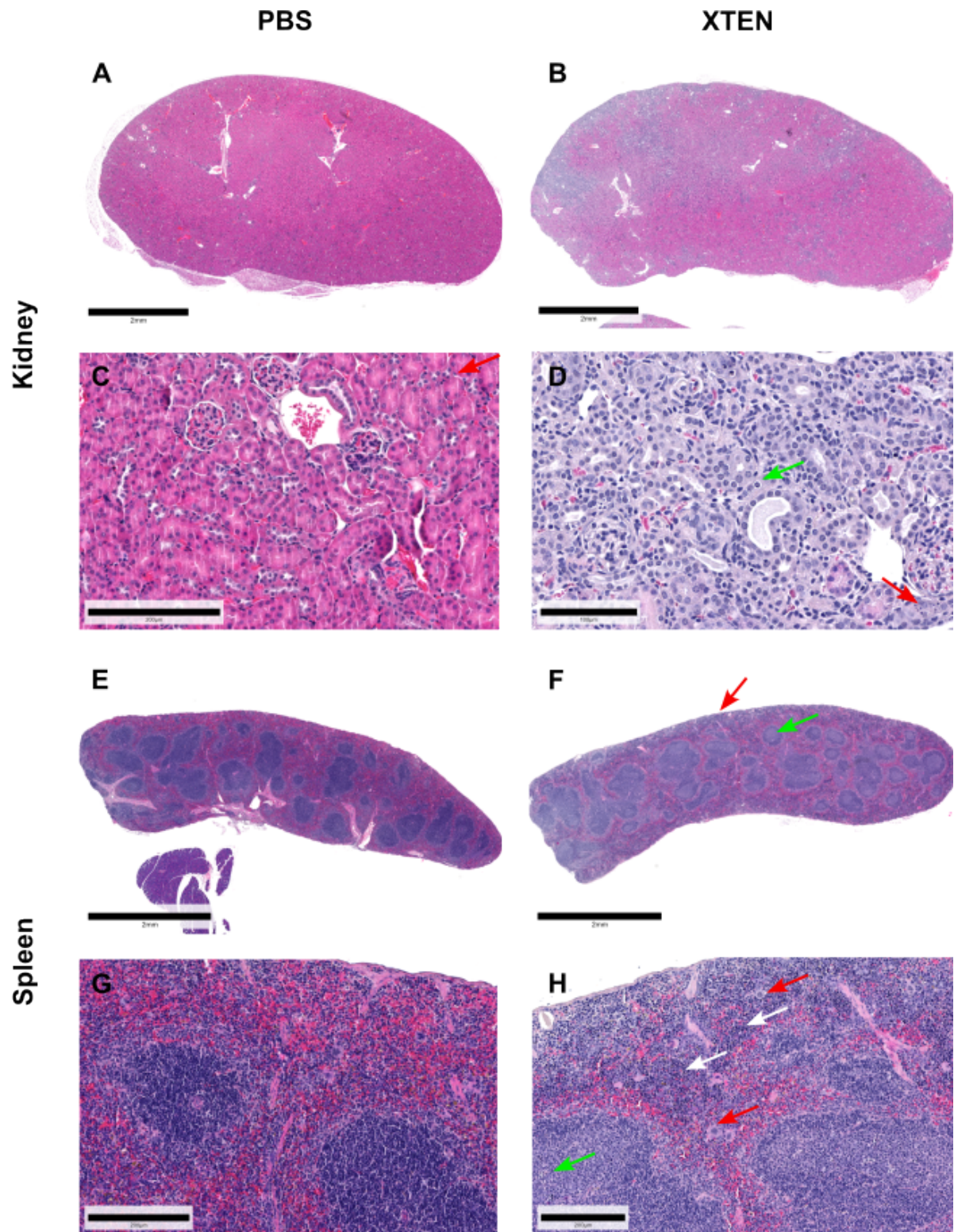


Supplemental Figure 19: Continuation of clinical chemistry testing results of C57BL/6 mice injected weekly with XTEN-*ReBphP*-PCM. Abbreviations: Bili-T = total bilirubin, TRIG = triglyceride, UIBC = unsaturated iron binding capacity, Na = sodium, K = potassium, Cl = chloride.



Supplemental Figure 20: Pathology of main organs for XTEN-*ReBphP*-PCM long-term injection study. BL6 mice were divided into two groups: 3 animals were injected intravenously with 0.75 mg of XTEN-*ReBphP*-PCM for 3 consecutive weeks, while the other three were injected with PBS. Mice were sacrificed after 3 weeks for blood (Suppl. Figure 16-19) and organ analysis. One mouse from the XTEN-*ReBphP*-PCM-injected group died prematurely after 2 weeks for unidentified reasons resulting in final group sizes of N=3 (PBS) and N=2 (XTEN).

H&E staining of Liver, heart, and lung from both PBS (Liver: exemplary **A**, see higher magnification in **C**; heart: exemplary **E**; lung: exemplary **G**) and XTEN-injected (Liver: exemplary **B**, see higher magnification in **D**; heart: exemplary **F**; lung: exemplary **H**) groups. All organs showed in no pathological alterations. Scalebars A, B, E, and F 2mm; C and D 200 μm ; G and H 500 μm . **For kidney and spleen see Suppl. Figure 20 continuation below.**

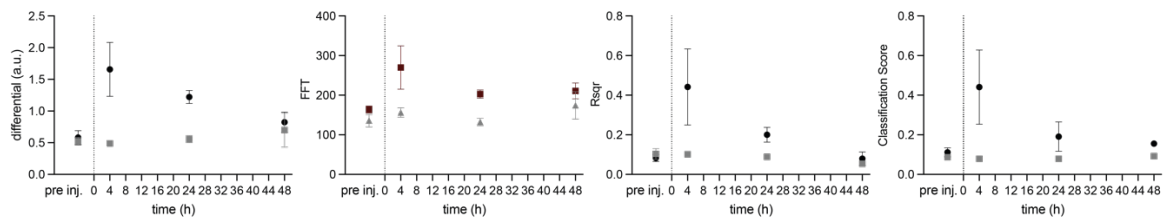
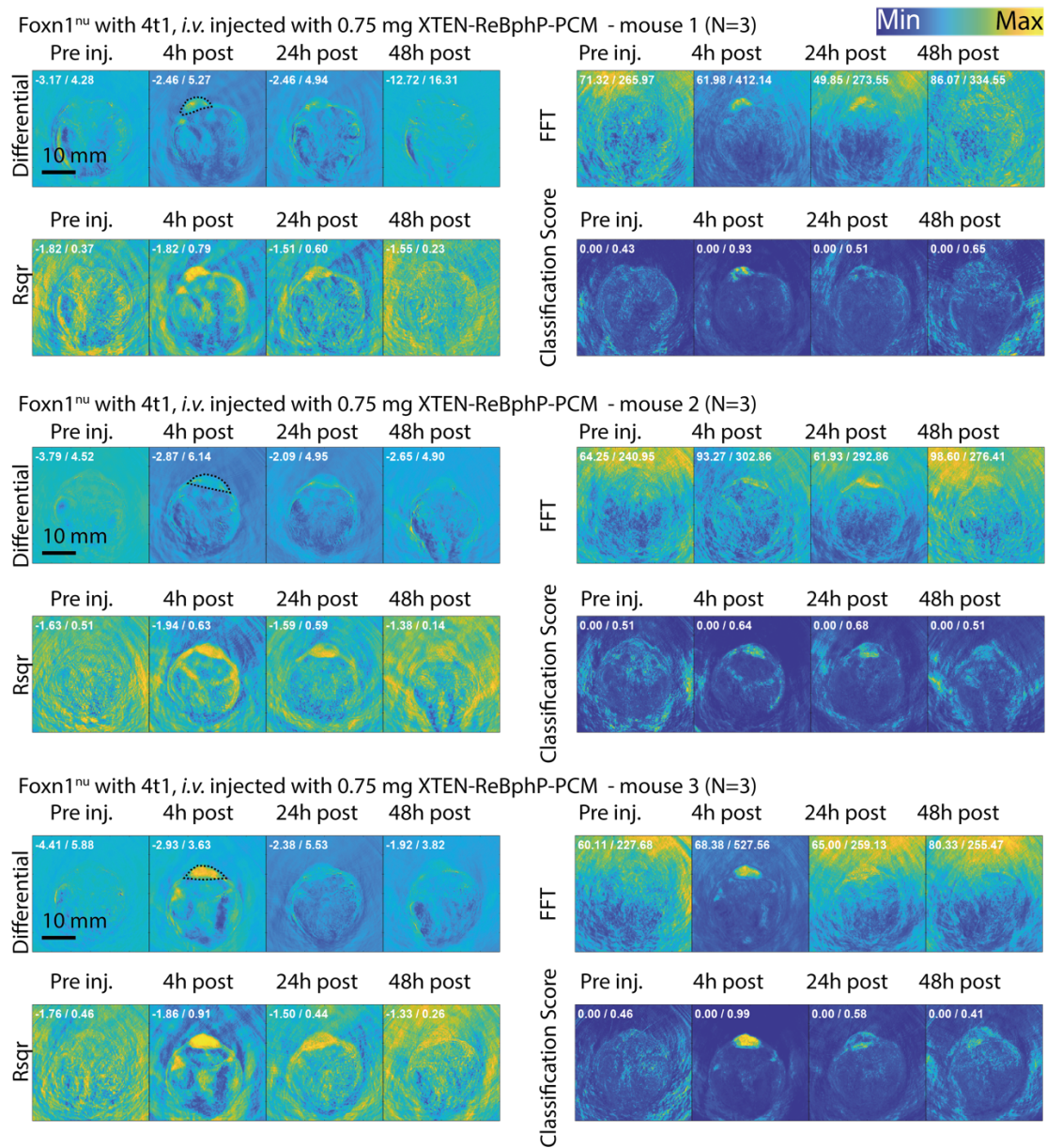


Supplemental Figure 20: Continuation of pathology of organs for XTEN-ReBphP-PCM long-term injection study. H&E staining of kidney tissues from all PBS-injected mice showed no pathological alterations (exemplary **A**, higher magnification in **C**), one XTEN-ReBphP-PCM-injected mice (**B**, higher magnification in **D**) showed a multifocal tubular basophilia. The affected regions displayed basophilic tubules, focal single cell necrosis (green arrow) and apoptosis (red arrow). The changes were mild, and the tissue retained a functional appearance

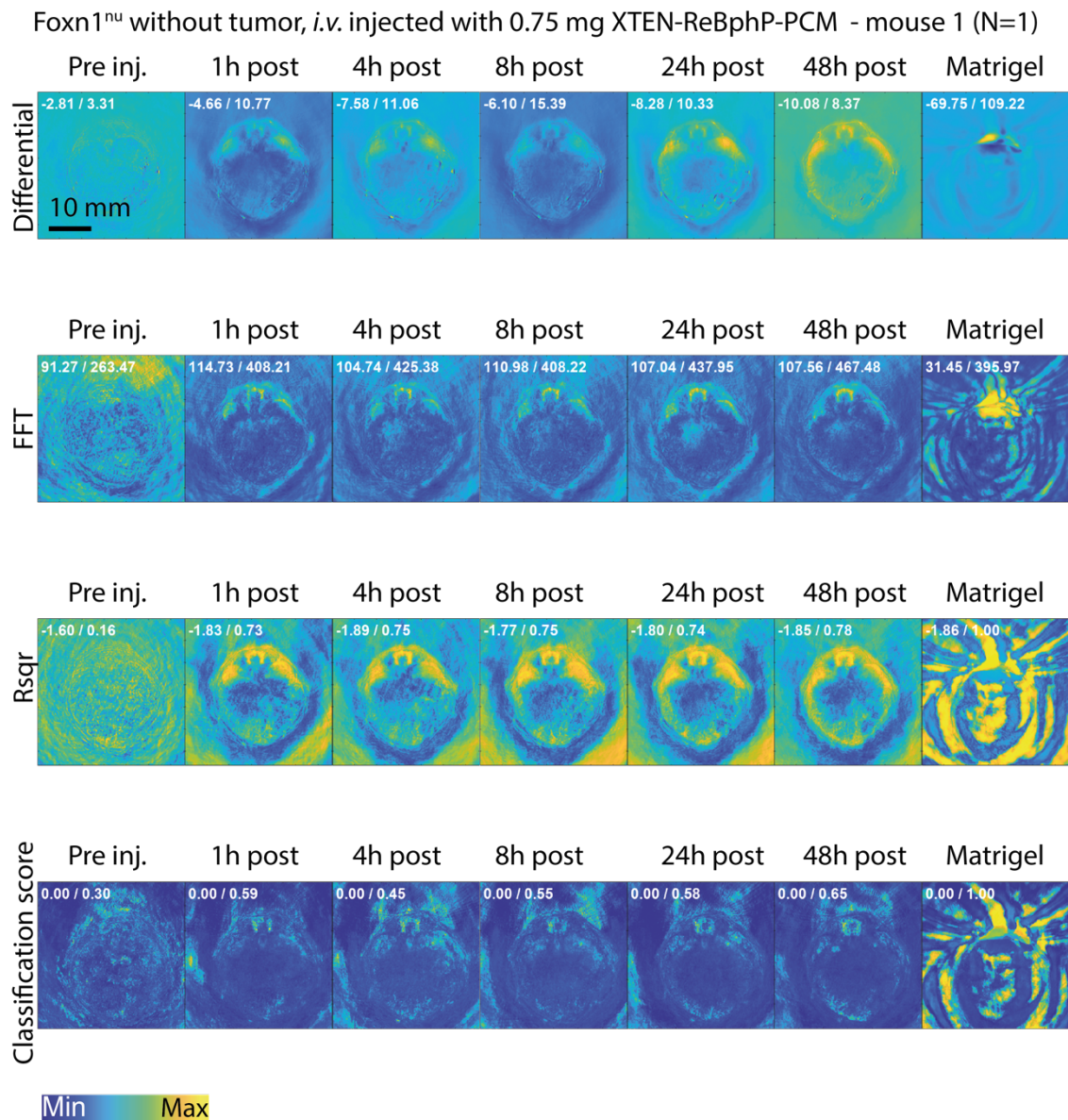
with no evidence of fibrotic or inflammatory. The other XTEN-injected mouse showed no pathological alternations in kidneys.

Spleen of PBS-injected mice showed no abnormalities (exemplary **E**, higher magnification in **G**), while those from both XTEN-injected mice (exemplary **F**, higher magnification in **H**) exhibited increased extramedullary hematopoiesis, characterized by a higher occurrence of megakaryocytes (red arrow), clusters of erythrocyte precursors (white arrow) and prominent splenic follicles with multiple apoptotic bodies (green arrow). Scalebars A, B, E and F 2 mm; C, G and H 200 μm ; D 100 μm .

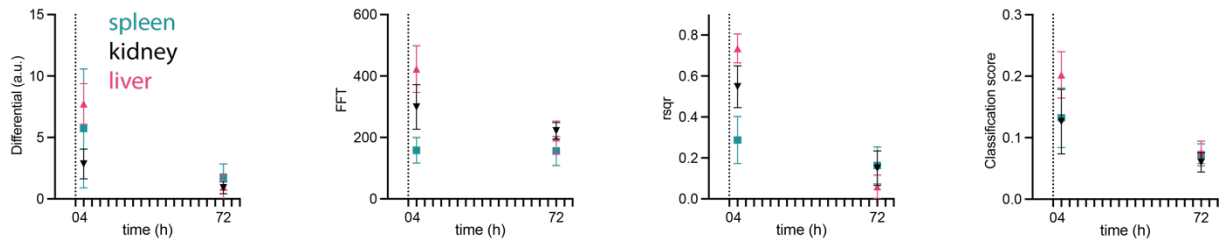
The mild group-specific differences in the spleen are possibly stress responses and correspond to the findings from the blood analysis (Suppl. Figure 16-19). The Tubular basophilia, that was observed in the kidney of one XTEN-injected mouse suggests renal regenerative changes potentially following an acute phase of tubule injury. These changes might correlate with the XTEN injection and reflected in the blood analysis data of this animal. Since these are mild regenerative changes that had no major impact on the organ function, a toxic effect of the XTEN injection seems unlikely.



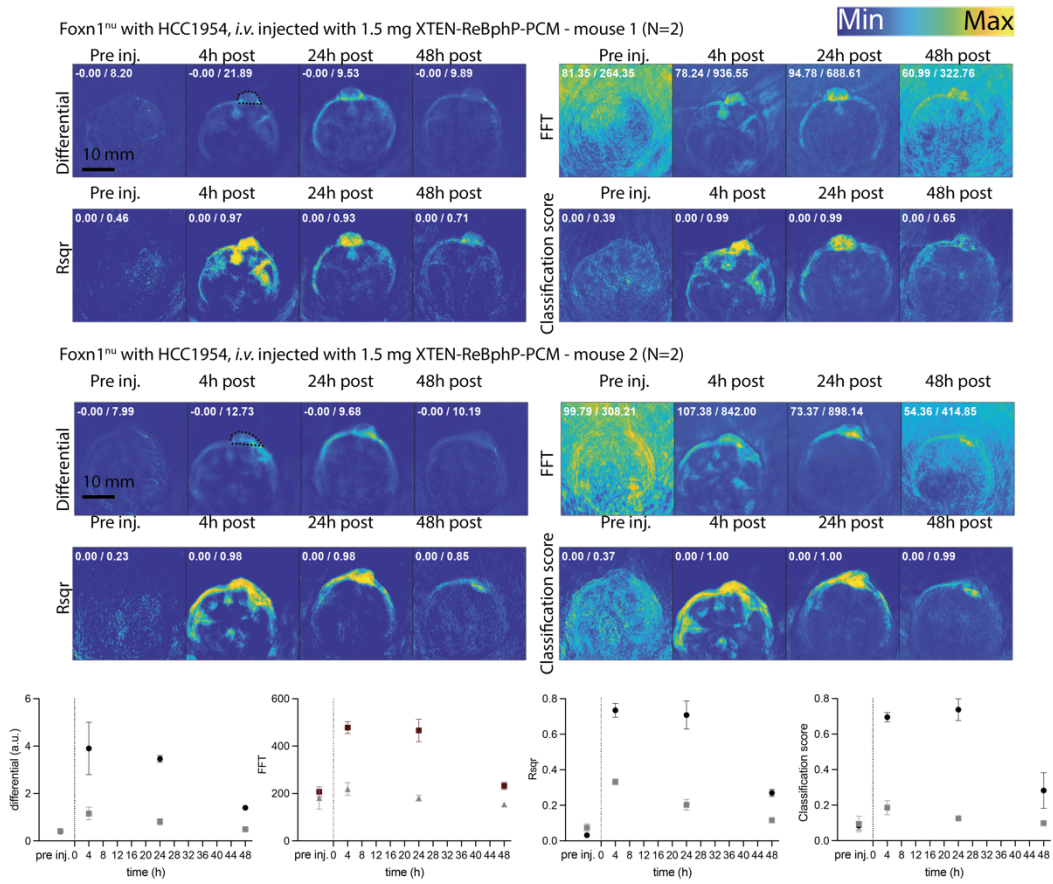
Supplemental Figure 21: Average intensity projections of 4T1-bearing mice injected *i.v.* with 0.75 mg XTEN-ReBphP-PCM. For each mouse (N=3) the average intensity projections of all measured slices are shown. For each projection the representation is scaled to min/max values (shown in the top left of each image) with the colorbar shown in the top right. To allow proper assessment of background and false positives (note negative rsqr values stem from the exponential fit not using an intercept; negative values in differentials mean a noise trend showing an increase). Tumor area is indicated by a dashed line on the 4h differential image. Additionally, mean (over the shown number of mice) and standard deviation are shown for the comparison between the tumor ROI (black) and the mouse ROI (outline of mouse, gray). Both ROIs are chosen on the maximum-intensity-projections at 770 nm. For the numerical analysis negative values for differential and rsqr are set to zero.



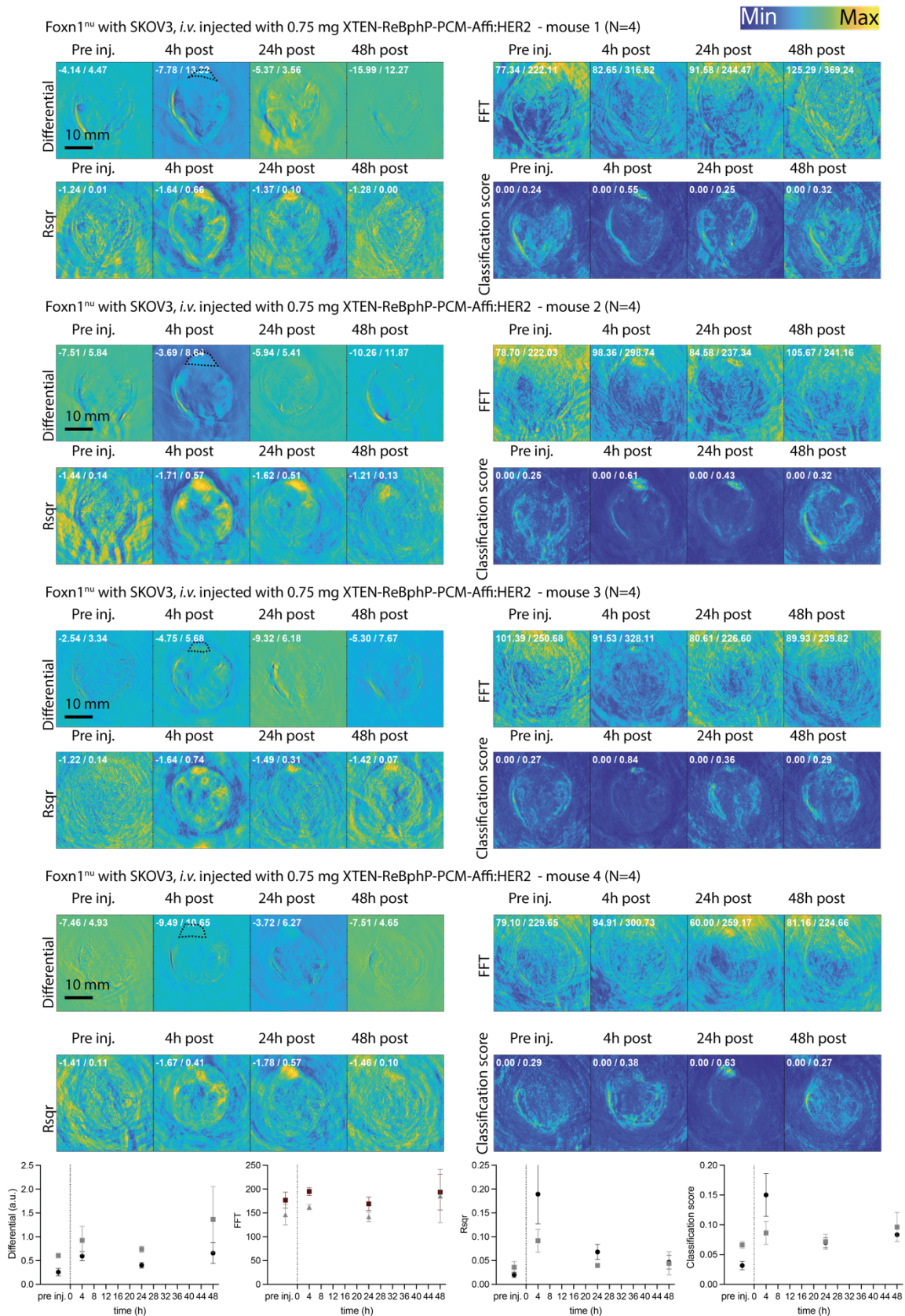
Supplemental Figure 22: Average intensity projections of mouse without tumor, injected *i.v.* with 0.75 mg of XTEN-ReBphP-PCM. The average intensity projections of all measured slices are shown. For each projection the representation is scaled to min/max (shown in the top left of each image) values to allow proper assessment of background and false positives (note negative rsqr values stem from the exponential fit not using an intercept; negative values in differentials mean a noise trend showing an increase). The colorbar is shown in the bottom left. After the last timepoint a dorsal Matrigel implant with a total of 0.25 mg XTEN-ReBphP-PCM was implanted as a positive control. Residual signals in the previous slices can stem from agent in blood and organs. The strong side lobe artefacts in the Matrigel control stem from bleeding out of the massive signal. In the Classification score those are especially visible in the out-of-mouse area since events not in the mouse were not included in the training data.



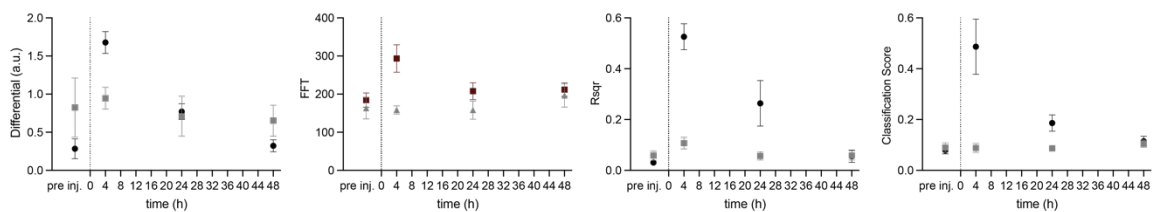
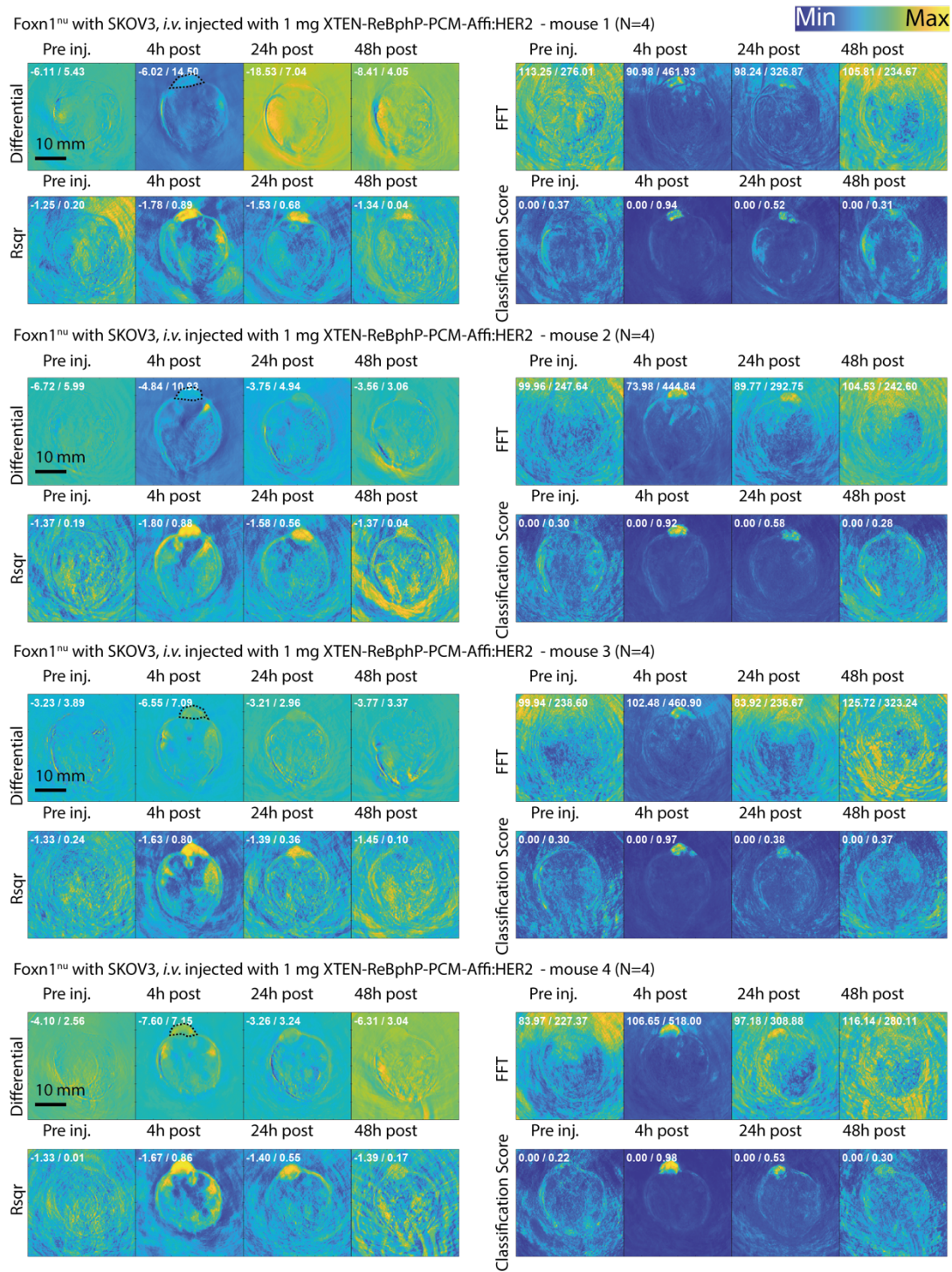
Supplemental Figure 23: Signals in organs following injection of 0.75mg XTEN-ReBphP-PCM in non-tumor C57Bl6J mice. Shown are the signal from liver, spleen, and kidney at 4 h and 72 h with organs from N=5 mice per timepoint.



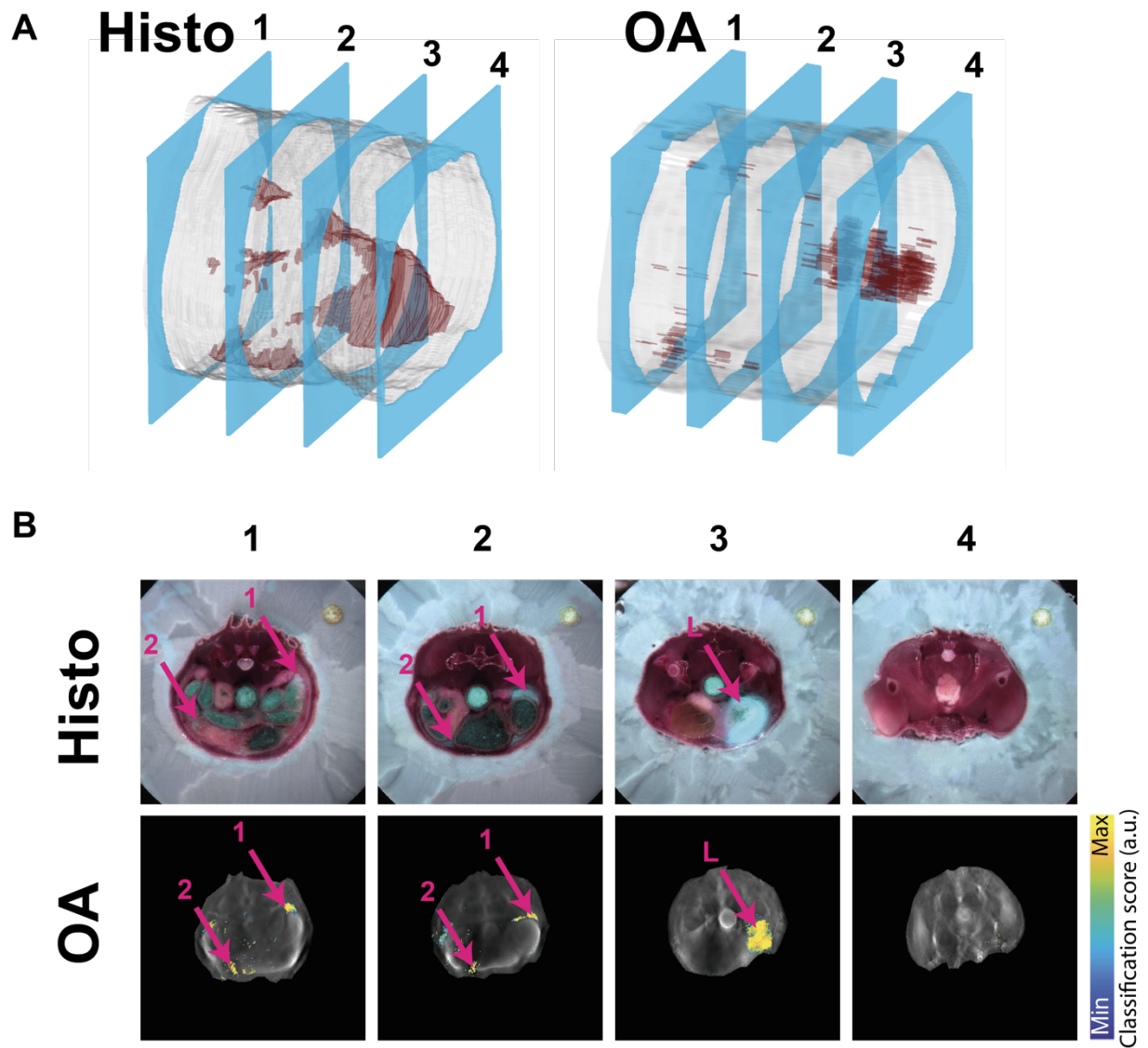
Supplemental Figure 25: Average intensity projections of HCC1954 s.c. bearing mice injected *i.v.* with 1.5 mg XTEN-ReBphP-PCM. Representation as in Suppl. Figure 21.



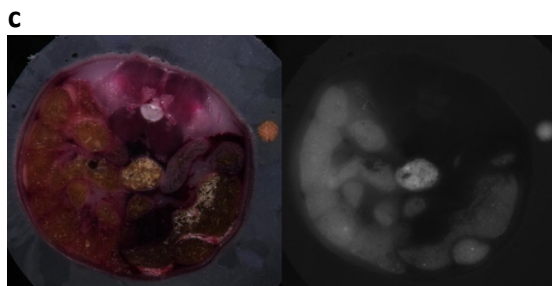
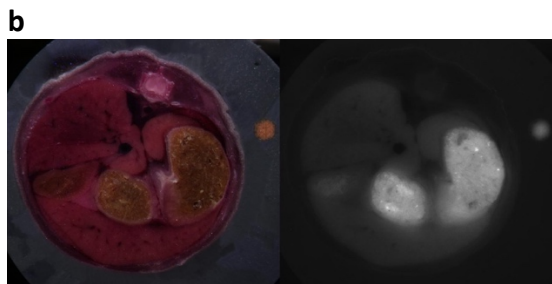
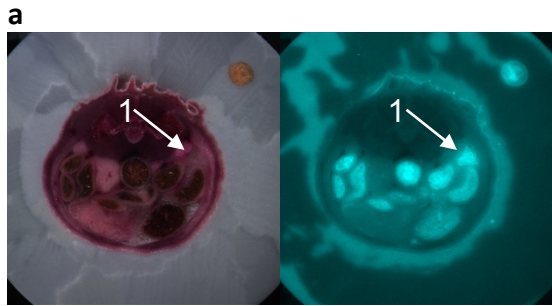
Supplemental Figure 26: Average intensity projections of s.c. SKOV3 bearing mice injected i.v. with 0.75 mg XTEN-ReBphP-PCM-Affi. For each mouse (N=4) the average intensity projections of all measured slices are shown. Representation as in Suppl. Figure 21.



Supplemental Figure 27: Average intensity projections of s.c. SKOV3 bearing mice injected *i.v.* with 1 mg XTEN-ReBphP-PCM-Affi. For each mouse (N=4) the average intensity projections of all measured slices are shown. Representation as in Suppl. Figure 21.



Supplemental Figure 28: Exemplary slices of the mouse volume shown in Figure 2f. **a** Histology and OA volume representations. Four corresponding representative slices are indicated on the volume in blue. **b** Slices of the volumes shown in **a**. Top row shows the overlay of brightfield and Cy5 channel, bottom row the OA unmixed with the representative slices colored by classification score, individually scaled to min/max with the colorbar indicated on the right. Note that the individual slices do not fully represent the same volume due to the differences in lateral focus.



Supplemental Figure 29: Individual channels of the histology composite image shown in Figure 2f and artefact autofluorescence from organs. **a** Brightfield channel (left) and Cy5 channel (right) for the composite histology image shown in figure 2f bottom right. The same tumor site is marked with arrow “1”. **b** Same representation as in **a** for a mouse without tumor and without agent injection. Shown is a slice in the stomach and liver region. **c** Same representation for a slice from the colon region. It is apparent that organs, especially colon and stomach with diet, show a signal in the Cy5 channel. Tumor vs. organ background can be faithfully identified by comparing the color and texture of the tissue in the brightfield image. While organs, especially colon / stomach containing diet, are rather strongly colored with distinct fine structure, tumor tissue is rather faintly colored and homogenous. Labeled tumor tissue is visible in the Cy5 channel often without clear boundaries – as opposed to organs. Moreover, organs show a more robust shape continuity through consecutive slices.

Bibliography

- 1 Orlova, A. *et al.* Tumor imaging using a picomolar affinity HER2 binding affibody molecule. *Cancer Res* **66**, 4339-4348 (2006). <https://doi.org:10.1158/0008-5472.CAN-05-3521>
- 2 Brandl, F., Busslinger, S., Zangemeister-Wittke, U. & Pluckthun, A. Optimizing the anti-tumor efficacy of protein-drug conjugates by engineering the molecular size and half-life. *J Control Release* **327**, 186-197 (2020). <https://doi.org:10.1016/j.jconrel.2020.08.004>